DEVELOPMENT OF GUIDELINES FOR THE AESTHETIC SURFACE TREATMENT OF SAFETY-SHAPED MEDIAN BARRIERS

A Thesis

by

JACOB RAYMOND NESS

Submitted to the Office of Graduate Studies of
Texas A&M University
in partial fulfillment of the requirements for the degree of

MASTER OF SCIENCE

August 2004

Major Subject: Civil Engineering

DEVELOPMENT OF GUIDELINES FOR THE AESTHETIC SURFACE TREATMENT OF SAFETY-SHAPED MEDIAN BARRIERS

A Thesis

by

JACOB RAYMOND NESS

Submitted to Texas A&M University
in partial fulfillment of the requirements
for the degree of

MASTER OF SCIENCE

Approved as to style and content by:

Harry L. Jones (Chair of Committee)	Lynn Beason (Member)
Harry Hogan (Member)	Paul N. Roschke (Head of Department)

August 2004

Major Subject: Civil Engineering

ABSTRACT

Development of Guidelines for the Aesthetic Surface Treatment of
Safety-Shaped Median Barriers.
(August 2004)

Jacob Raymond Ness, B.S., Texas A&M University
Chair of Advisory Committee: Dr. Harry L. Jones

Safety-shaped median barriers have long been employed to keep misguided vehicles on the roadway. In recent years there has been a growing national desire for more aesthetically pleasing roadside safety systems. Adding surface texture is one of the most popular ways to make a more aesthetically pleasing barrier. This practice of adding surface texture can potentially reduce the safety performance of the barrier.

The purpose of this research was to develop guidelines for the aesthetic surface treatment of safety-shaped median barriers. Numerical simulation was utilized to develop these guidelines. This was done by first validating the vehicle model that was used in this research, which was the National Crash Analysis Center (NCAC) 2000P Detailed Pickup Truck model. The validity of the vehicle model could be determined by comparing the vehicle dynamics of the simulation to the actual crash test data for the smooth surfaced Single Slope and New Jersey Safety-Shaped barriers. Crash tests involving concrete median barriers most commonly fail crash testing criteria given by the National Cooperative Highway Research Program (NCHRP) *Report 350* by excessive Occupant Compartment Deformation (OCD). OCD is excessive deformation of the occupant compartment that would cause severe harm to the occupant. Current simulation vehicle models do not give reliable direct measurement of OCD. To take the place of direct measurement, several parameters were measured to find the best surrogate measure of OCD. The internal energy of the floorboard in the NCAC 2000P Detailed Pickup Truck model gave the best correlation to OCD. By simulating several different past crash tests with passing and failing OCD, limits of internal energy in the floorboard could determine if a simulation had passing, marginal, or failing amounts of OCD.

Using the surrogate measure of OCD a parametric study was then evaluated by NCHRP *Report 350* standards. The parametric study of 29 simulations varied width and depth of recess between asperities for two different angles of asperities. Guidelines were determined for the 45° and 90° angles of asperities as a curve on depth vs. width of recess between asperities from the results of this parametric study.

ACKNOWLEDGMENTS

Support for this project was provided by the National Cooperative Highway Research Program through the Texas Transportation Institute's Center of Excellence in Transportation Computational Mechanics. I would like to thank the many people who helped in completing this research. A special thanks goes to Dr. Harry Jones for his time and effort throughout my academic career and to Mr. Lance Bullard, Dr. Roger Bligh, Dr. Akram Abu-Odeh, and Mr. Nauman Sheikh for their significant guidance throughout this research.

Finally, I would like to thank my wife, Daniele, for her support and encouragement, which have helped make this accomplishment possible.

TABLE OF CONTENTS

Page

Page

LIST OF FIGURES

LIST OF TABLES

TABLE Page

1. INTRODUCTION

1.1 BACKGROUND

In recent years there has been a growing national desire for more aesthetically pleasing roadside safety systems. To meet this growing demand, several state departments of transportation have developed aesthetic surface designs. One of the most popular ways to make a more aesthetically pleasing barrier is by adding surface relief and texture (see Fig. 1). Since adding surface texture to a roadside safety system is a relatively new and untested concept, most designs have been based solely on engineering judgment. Designers are in need of recommendations or guidelines to give them boundaries that they can work within with some degree of confidence. Without guidelines to limit the geometry of the surface relief, the designer could inadvertently create a surface with the potential for dangerous interaction with a vehicle in the event of a crash.

The purpose of this research was to develop guidelines for the aesthetic surface treatment of safety-shaped median barriers. These guidelines are intended to ensure that

FIG. 1. Aesthetic Concrete Barrier (White et al. 2002)

This thesis follows the style and format of the *Journal of Transportation Engineering*, ASCE.

aesthetic treatments to safety-shaped concrete barriers do not adversely affect the safety performance of the barrier when struck by an errant vehicle. An example of a safety-shaped barrier profile, called the New Jersey Safety-Shaped Barrier is shown in Fig. 2. The New Jersey Safety-Shaped barrier is the most demanding of the safety-shaped barrier profiles due to size of the toe of the barrier, which is the lower section of the barrier profile that the front tire often climbs in a crash event. The New Jersey Safety-Shaped barrier was the primary barrier profile used in this research.

Due to the lack of design guidelines at the national level, there is currently no uniformity in aesthetic barrier design among the States. Variables involved in adding surface texture to median barriers include, but are not limited to, the type of median barrier, and the depth, width, and shape of the relief or recess. Due to the number and range of these variables, it would be impractical to conduct a parametric investigation based solely on crash testing. However, such

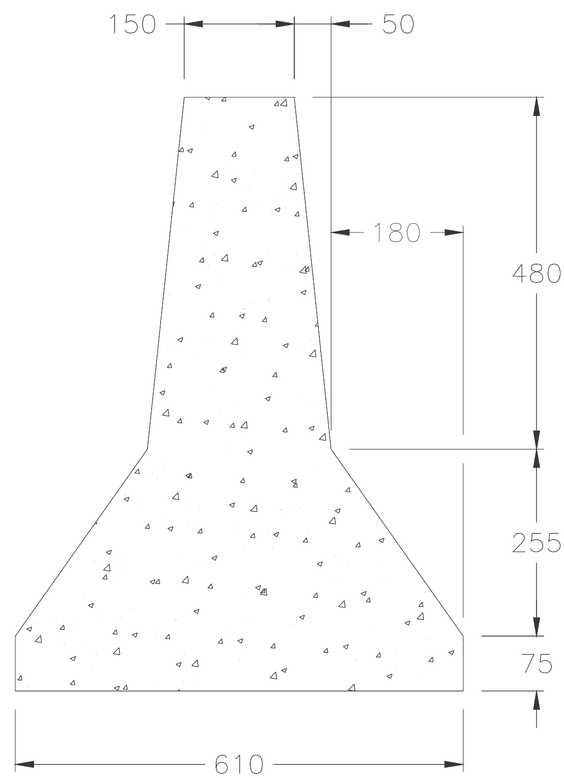

FIG. 2. New Jersey Safety-Shaped Barrier

problems lend themselves to analysis and evaluation through computer simulation. Therefore, the research approach used to evaluate the effect of aesthetic surface treatments on concrete median barriers utilizes a combined program of finite element analysis (FEA) and full-scale crash testing.

The simulation effort was intended to provide a detailed assessment of the three-dimensional impact response of a specific aesthetic treatment. A series of computer simulations were conducted on selected treatments following impact conditions similar to those recommended for the evaluation of longitudinal barriers in National Cooperative Highway Research Program (NCHRP) *Report 350*. This standard governs federal crash test performance requirements for roadside safety systems on the National Highway System (Ross et al. 1993).

1.2 HISTORY OF ROADSIDE SAFETY ENGINEERING

Most components of the highway design procedure were developed in the late 1940s and the 1950s. Since roadside safety design was established as a component of highway design in the 1960s it is a relatively new concept (AASHTO 1996). Prior to 1960, public policy regarding roadside safety focused on the responsibility of each driver to keep out of danger. If a vehicle were to leave the roadway, the “nut behind the wheel” would have to deal with the consequences (Ross 1995). Accordingly, roadside appurtenances were often constructed to resist impact forces of collision with a vehicle without regard to safety of the motorist. Fixed-base light posts, rigid telephone poles, and unyielding bridge supports within several meters of the roadway were common. Because the signpost was not designed to minimize damage to a vehicle during a collision, the consequences of a seemingly minor collision were severe to motorist, signpost, and vehicle. This “nut behind the wheel” philosophy led to dangerous roadsides. United States fatality rates per one hundred million vehicle miles in 1930 were more than 1,000% what they were by 1998 (National Safety Council 1998). In the 1960’s, serious concerns about roadside safety led highway engineers to adopt a “forgiving roadside” concept for highway design. With an ever-increasing number of fatalities caused by dangerous roadways, public sentiment pressured lawmakers to make changes. A nine-meter “safe zone” was introduced to put distance between roadside obstructions and the flow of traffic. In the event that an obstruction could not be removed from the safe zone, roadside safety devices were designed to either shield the obstruction from vehicle impact or to break away upon impact. Engineers began to design roadsides with the intent of protecting vehicle occupants in the event that a vehicle was to leave the roadway. Through innovations such as slip base sign supports, impact attenuating crash cushions, and redirecting guardrails, both the frequency and severity of roadside collisions has decreased significantly (Ross 1995). Despite the advances in technology and changes in philosophy, there still exists room for improvement.

FIG. 3. Single Slope Barrier with Unacceptable Surface Geometry (White et al. 2002)

Both the Federal Highway Administration (FHWA) and state departments of transportation such as the Texas Department of Transportation (TXDOT) invest significant resources into developing better roadside devices and investigating the safety of current practices. By upgrading outdated facilities and implementing new technologies when possible, the safety of roadways can improve dramatically. In this research, the effects of aesthetic surface treatments on safety-shaped barriers was evaluated through crash testing and numerical simulation in order to verify compliance with current safety performance standards. Fig. 3 shows an example of a surface treated barrier, which failed to meet NCHRP *Report 350* requirements. The failure was caused by a lack of guidance for the relief of the surface geometry. This research attempts to give guidance to designers in this situation working with safety-shaped barriers.

1.3 STATE OF PRACTICE

Over the last several decades the general public has begun to push for more aesthetically pleasing roadside safety systems. One of the ways a roadside safety system can be made more aesthetically pleasing is by changing the overall geometry of the barrier. When overall geometry of a roadside safety system is changed it must be reevaluated with crash testing to meet NCHRP *Report 350* standards. The most cost effective approach to making a

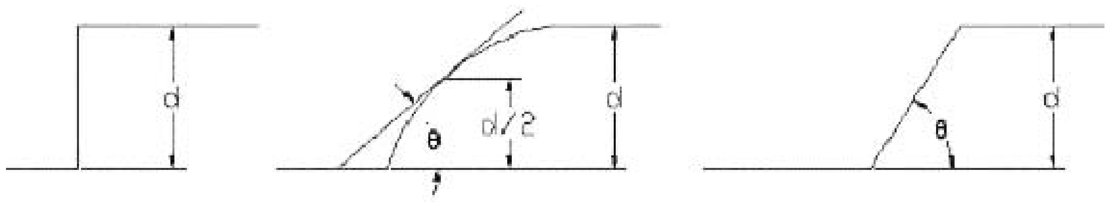

(a) (b) (c)

FIG. 4. Surface Asperities: (a) Perpendicular; (b) Rounded; (c) Angled

barrier more aesthetic is to put a new surface treatment on a proven barrier profile. The surface treatment makes the barrier more aesthetic by appearing to be part of the natural environment or by using light and shadow contrasts. States have been allowing modest surface treatments to be used on barriers for the past few years. As the surface treatments have become more complex, the departments of transportation have grown concerned with a possible loss in performance of these barriers.

Almost all surface asperities can be placed within one of three categories: Perpendicular, Rounded, or Angled Surface Asperities. These generalized types of surface asperities are shown in Fig. 4. The angled or inclined asperity can be defined in terms of a depth "d" and angle "θ," either of which can be varied in order to achieve a different profile. The perpendicular asperity is a subset of the angled asperity with θ = 90 degrees. The rounded asperity can be approximated as an angled surface asperity by selecting an effective angle θ. The illustration shown in Fig. 4 uses a tangent to the rounded surface at half the depth "d" to define an effective angle "θ." Because the angled asperity is the most general, it was the type of surface asperity used in the parametric study to develop guidelines for the aesthetic treatment of concrete median barriers.

1.4 LITERATURE REVIEW

1.4.1 Standards for Roadside Safety Devices

Roadside safety engineers have long employed destructive full-scale crash testing to evaluate performance of roadside safety devices. In order to establish a set of standard criteria for these tests, FHWA recently adopted the guidelines presented in NCHRP *Report 350* (Ross et al. 1993) to evaluate roadside safety devices. In addition, FHWA requires that all new roadside features installed on the National Highway System after September 1998 meet NCHRP *Report 350* recommended safety performance guidelines. The safety performance of a roadside appurtenance is evaluated by three factors in accordance with NCHRP *Report 350*. The structural adequacy of the roadside feature, the occupant risk during the event, and the post-impact vehicular response are criteria used to judge the performance of a proposed system.

Several evaluation criteria must be satisfied in order for a safety feature to perform successfully with respect to structural adequacy. First, a guardrail or barrier test device should contain and redirect the vehicle. Moreover, during redirection the vehicle should not penetrate, under run, or override the installation. When a breakaway or slip base is being tested, the device should readily activate in a predictable manner by breaking away, fracturing, or yielding as intended. Finally, for crash attenuating systems, acceptable performance can be redirection, controlled penetration, or controlled stopping of the vehicle. For the case of concrete median barriers, only the first of these criteria apply. This research assumes that the barrier has been adequately designed for strength.

The second major NCHRP *Report 350* criterion is occupant risk. Fragments and debris resulting from the collision should not penetrate the occupant compartment or present a hazard to pedestrians, workers in a work zone, or other motorists. The occupant compartment should also not be damaged through excessive deformation in such a way that occupant injury is likely. Deformation measurements of the occupant compartment are used to create a damage index, which is explained in Appendix E of NCHRP *Report 350*. The report shows the locations of these various measurements. In NCHRP *Report 350* results are quantified in terms of percent change in length, but the roadside safety community now uses a pass/fail criterion, based on the change in length of a value of 150 mm dimension. Other reasons for failure can be as simple as a shattered windshield or excessive localized deformation that shows signs of causing significant injury to the occupant. Although the risk of occupant injury during a vehicle collision is highly dependant upon the crashworthiness of the vehicle, NCHRP *Report 350* removes the variability of vehicular crashworthiness in evaluating the performance of roadside safety features. Gross vehicle accelerations are used as one indicator of occupant risk because they are directly due to the interaction between the vehicle and the test device. Changing the properties of the roadside safety device can alter accelerations experienced by motorists during an impact event. Using the flail space model presented in Appendix A of NCHRP *Report 350*, gross vehicle accelerations are used to calculate occupant impact velocity (OIV) and ridedown acceleration, the two parameters used to relate gross vehicle accelerations to occupant risk. Ranges of these values for acceptable performance are given in NCHRP *Report 350*.

The final criterion used to judge the performance of roadside safety devices is the after collision vehicle behavior. After a collision, the impacting vehicle cannot enter adjacent or oncoming lanes of traffic. Also, the exit angle of the vehicle from the system must be less than 60°. Finally, limits are placed on the OIV and ridedown acceleration while the vehicle comes to a stop after impacting the test system (Ross et al. 1993).

1.4.2 Existing Guidelines

Crash testing of Single Slope median barrier with aesthetic surface treatments by California Department of Transportation (CalTrans) resulted in the first set of guidelines for the aesthetic surface treatment of concrete barriers (White et al. 2002). As a result of the CalTrans study and subsequent approval by the FHWA, allowable surface asperity recommendations for Single Slope and Vertical Face barriers set out by CalTrans in September 2002 and FHWA in December 2002 were as follows:

1. Sandblasted textures with a maximum relief of 9.5mm
2. Images or geometric patterns into the face of the barrier 25 mm or less and having 45˚ or flatter chamfered or beveled edges to minimize vehicular sheet metal or wheel snagging.
3. Textures or patterns of any shape and length inset into the face of the barrier up to 13 mm deep and 25 mm in width. Geometric insets with an upstream edge with an angle of up to 90˚ should be less than 13mm.
4. Any pattern or texture with gradual undulations that have a maximum relief of 20 mm over a distance of 300 mm.
5. Gaps, slots, grooves, or joints of any depth with a maximum width of 20mm and a maximum surface differential across these features of 5 mm or less.
6. No patterns shall feature a repeating upward sloping edge or ridge.
7. Any pattern or texture with a maximum relief of 64 mm, if such pattern begins 610 mm or higher above the base of the barrier and all leading edges are rounded or sloped to minimize any vehicle snagging potential. No part of this pattern or texture should protrude below the plane of the lower, untextured portion of the barrier.

Prior to the CalTrans study there was a lack of aesthetic guidelines at the national level and, little or no uniformity in aesthetic barrier design among the States. CalTrans recommendations listed as 2 and 3 most closely paralleled guidelines developed by this project. These recommend a maximum depth of 25 mm for surface asperities featuring a 45˚ angle to upstream traffic and 13 mm for surface asperities featuring a 90˚ angle to upstream traffic to designers. The CalTrans study provides design guidance for Single Slope and Vertical Faced concrete barriers. However, guidance of a similar nature such as the depth, width, and shape of the surface relief or recess is needed for safety-shaped barriers.

1.5 FINITE ELEMENT SIMULATION

The program that was utilized for the computer modeling effort was LS-DYNA (2001). LS-DYNA is a general-purpose, explicit finite element code used to analyze the nonlinear dynamic response of three-dimensional inelastic structures. The finite element models used utilize both 4-noded shell elements and 8-noded solid elements (Hallquist 1998). Over the last 8 years, LS-DYNA has been used extensively in the simulation of crash testing of roadside safety barriers. Since the barriers used in studies such as this are restrained concrete barriers and bridge rails, which are being modeled with a rigid material, future improvements in the accuracy of simulated crash events will be made through improved representation of various components of the vehicle model. As explained in Section 3, an inadequate finite element representation of the small car vehicle model led to difficulties in developing the guidelines.

1.6 SUMMARY

The national need for guidelines for the surface treatment of safety-shaped barriers was discussed. The basic approach necessary for designers to make roadside safety systems more aesthetically pleasing is through geometric changes to the system or to add a surface treatment. Variables of the perpendicular, rounded, or angled surface textures were defined. Existing guidelines for the Single Slope Barrier were presented. The goal of this research was to develop guidelines for the aesthetic surface treatment of safety-shaped barriers. Background was given on the finite element analysis software, LS-DYNA, which was used in this research.

2. RESEARCH METHODOLOGY

2.1 OVERVIEW

In the previous section, the problem of developing guidelines for limiting depth and width of aesthetic surface treatments on safety-shaped barriers was discussed. The standard for roadside safety devices, NCHRP *Report 350*, was also discussed. In order for a roadside barrier to comply with NCHRP *Report 350* guidelines, it must pass a series of full-scale crash tests; the most demanding test is the 100 km/hr (62 mph) impact of a full-sized, 2,000 kg (4,400 lb) pickup truck (2000P) with the barrier at an angle of 25°. Another test in this series is the test of a 820 kg (1,804 lb) small car (820C) at 100 km/hr (62 mph) with the barrier at an angle of 20°. The small car crash test evaluates the system for vehicle stability and system stiffness, while the pickup truck crash test evaluates the system strength. As seen in Fig. 5, a full-scale crash test requires an extensive setup, instrumentation, and destruction of a test vehicle. The cost per test is substantial. The research plan that was used to develop guidelines for the aesthetic surface treatment of safety-shaped median barriers focuses on validating vehicle models, finding a surrogate measure of Occupant Compartment Deformation (OCD), and evaluating a parametric study using FEA. Each step in this research plan is discussed briefly in this section.

FIG. 5. Full-Scale Crash Test

Implementation of the test plan and results from the tests performed for this research are presented later.

2.2 VEHICLE MODEL VALIDATION

Crash tests were simulated using LS-DYNA and two finite element vehicle models that were developed by the National Crash Analysis Center (NCAC). One of the models, the 820C small car, is a representation of a Geo Metro with 20,000 elements. The other NCAC model was the Detailed Pickup Truck, which uses more than 56,000 elements to represent a Chevrolet C2500. Both vehicle models are shown in Fig. 6. The finite element models of these vehicles are available to the public through the Public Finite Element Model Archive (2004) hosted by NCAC. LS-DYNA also contains a large library of material models, meshing patterns, contact algorithms, and element formulations that permit a good representation of the concrete barrier system.

To examine the suitability of the two NCAC vehicle models for use in this study, several validating simulations were performed using basic rigid barrier profiles. Collision of the 820C small car model with a Single Slope barrier was also simulated because the surface treatment

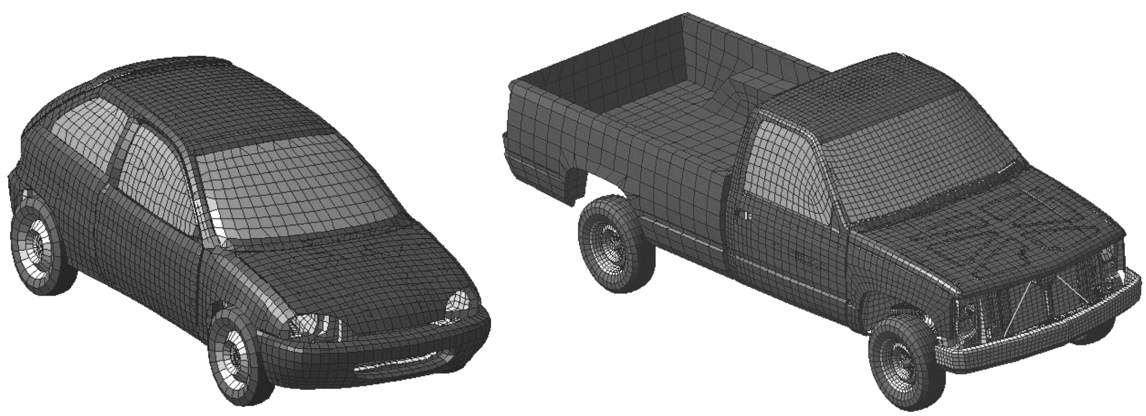

(a) (b)

FIG. 6. Vehicle Models: (a) 820C Small Car; (b) 2000P Pickup Truck

was observed to produce a rolling behavior in an actual crash test. This barrier is discussed in more detail in the next section. Early in the evaluation of the validity of simulations with the vehicle models used in this study, it became apparent that the 820C small car vehicle model required suspension and tire model improvements. In several simulations of past actual crash tests, vehicle climb and deformation was severely underestimated by the simulations. This was attributed to rigid suspension components and a coarsely meshed tire. The 2000P pickup truck model, on the other hand, gave consistent and reasonable behavior, suggesting that satisfactory results could be obtained with the suspension elements incorporated within this vehicle model.

2.3 SURROGATE MEASURE OF OCD STUDY

Using FEA, a study was conducted to determine if a surrogate measure can be defined to quantify the outcome of a passed, marginal, or failed crash test based on OCD. Several past crash tests of concrete barriers with the 2000P pickup truck were identified. All of the identified crash tests were modeled and simulated using LS-DYNA. Each simulation was setup to collect several potential surrogate measures of OCD. A surrogate measure is a quantitative parameter, which can be evaluated in place of another parameter such as OCD that cannot be measured with adequate consistency. The potential surrogate measure that showed the best correlation with maximum OCD reported in the crash tests was selected.

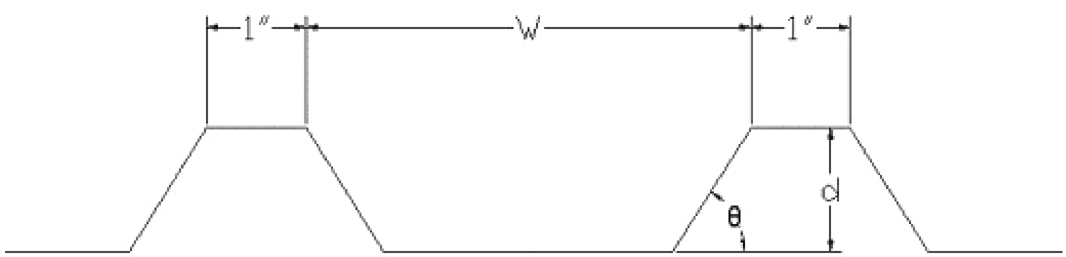

FIG. 7. Parametric Study Variables of the Angled Asperity Surface Profile

2.4 PARAMETRIC STUDY

In this research a parametric study of the variables of angled asperities were used. As seen in Fig. 7, an angled asperity is comprised of a depth “d”, width “W”, and angle “θ.” Angled asperities were chosen for their clearly defined variables, which can be easily interpreted by a designer. Few aesthetic designs in use today have as simple a geometry as the angled asperity used in the parametric study, but a designer can use a conservative estimate of depth, width, and angle for their surface geometry.

To make the parametric study as efficient as possible the relationship between depth and width of a surface geometry on barrier performance had to be well understood. For a given angle “θ,” the relationship between the depth of recess “d” and width of recess “W” can be conceptualized as shown in Fig. 8. The region below the curves would constitute acceptable asperity geometry while the region above these curves would constitute unacceptable geometry. It can be seen that once “W” becomes large enough, there is a depth “d” at which the vehicle’s impact path will only intersect a single asperity and the curve flattens out into a horizontal line.

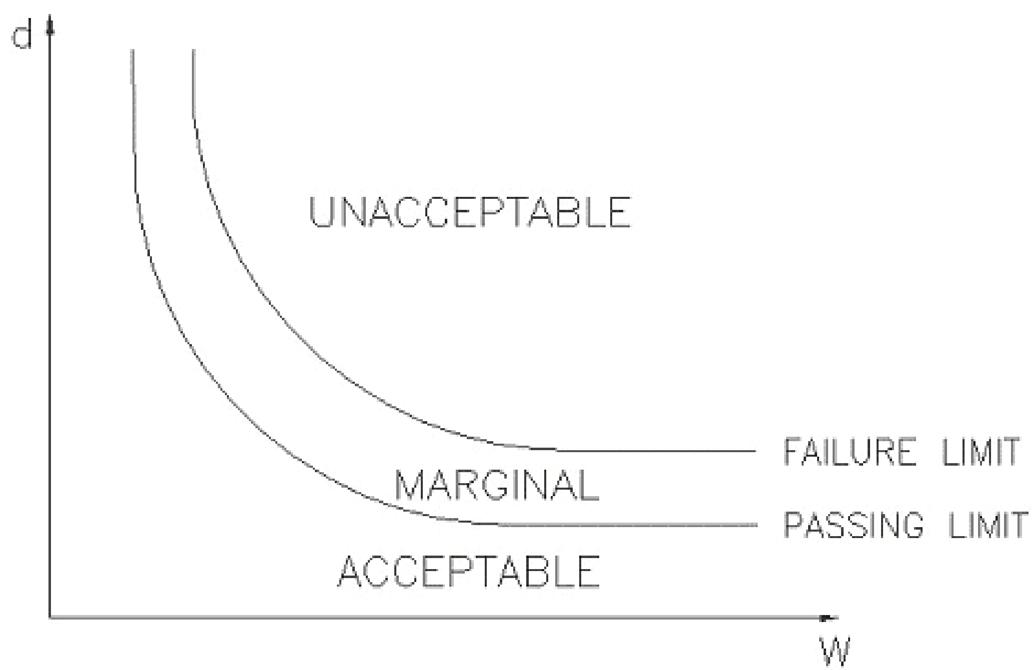

FIG. 8. Conceptual Relationship between Recess Depth and Width

As “W” decreases, there is a value at which the spacing of the asperities is sufficiently narrow to prevent vehicle contact with the full depth of the recess, therefore the acceptable value of “d” increases. In this study a predetermined set of simulations to make up the parametric study was not possible because the relationship between depth and width was not well known. As each simulation of the parametric study progressed the curves took form and future simulations were adjusted to get the most out of each simulation.

2.4.1 Failure Criteria

2.4.1.1 Vehicle Stability

To evaluate the parametric study there was a need for measures by which a passing or failing simulation could be determined. Vehicle stability is when a vehicle in a crash test rolls over or shows the potential to roll over. Using the 820C small car vehicle the most critical criterion to check for is vehicle stability on safety-shaped barriers. Many early designs induced rollover of the small car by the barrier’s toe. There are several safety-shaped barrier profiles in use today, but the New Jersey Safety-Shaped Barrier is generally viewed as the most likely to cause vehicle stability problems with a small car because of its prominent toe. It was therefore used in the evaluation of the parametric study.

2.4.1.2 Occupant Compartment Deformation

OCD is a measure of the amount of deformation into the vehicle’s occupant compartment. This criterion is important because in some crash tests the vehicle had acceptable occupant risk values such as occupant impact velocities and ridedown acceleration, but the occupant’s limbs were sometimes severely injured due to excessive crushing of the occupant compartment (Buth et al. 1998a). OCD was recognized in NCHRP *Report 230*, but was introduced quantitatively into crash testing evaluation criteria in NCHRP *Report 350*. Excessive OCD is a common cause of failure in concrete barrier crash tests using the 2000P pickup truck.

2.5 CREATING A CRASH SIMULATION

Simulating the impact of a vehicle with a barrier involves three distinct activities: preprocessing, processing, and postprocessing. First, preprocessing uses the geometric data given on engineering design drawings to build the model. This was done using the preprocessor Hypermesh (2001). Hypermesh (version 5.0) is a product of Altair, Inc., and can be used to define model geometry, finite element mesh, and loading and boundary conditions. Once the barrier model was developed, an input file for the FEA code LS-DYNA (2001) was exported from Hypermesh. A vehicle model can now be inserted into the input file at the end of the barrier input using any standard text editor. This is the start of the processing stage where LS-DYNA runs the model input file. LS-DYNA is a general-purpose commercially available finite element code capable of nonlinear, explicit analysis of dynamic events. Dynamic structural analysis of the impact event is simulated in LS-DYNA using the input file from Hypermesh. Finally, LS-POST (2001) and Altair Hyperview (2001) are used to postprocess results of the finite element analysis. LS-POST is used to filter ASCII data files. Hyperview, with superior rendering capabilities, is used to view graphical output of deformed shapes at discrete time steps. These postprocessing packages were used to display and analyze a simulation graphically to help find possible errors in the model. Numerical simulation for this research is performed on a four processor Compaq Alphaserver ES40, on two dual-processor Pentium III Dell workstations, and on two dual-processor Xeon Dell workstations. These computers are owned and maintained by the Safety and Structural Systems Division at the Texas Transportation Institute (TTI).

3. VEHICLE MODEL VALIDATION

3.1 OVERVIEW

To have confidence in results produced by FEA simulation the components of the model must be first validated. The two primary models in a crash simulation are the vehicle and barrier. The barrier model is represented as a rigid surface, which leaves only the vehicle model with the need for validation. The vehicle model is either the 820C small car or 2000P pickup truck. Each of these vehicle models have been used extensively in the area of roadside safety. To validate a vehicle model, previous crash tests were simulated and the vehicle dynamics were compared in terms of vehicle roll, pitch, and yaw.

3.2 820C VEHICLE VALIDATION

To validate the 820C vehicle model, three past crash tests were simulated. These crash tests involved the Fluted Single Slope barrier, the smooth Single Slope barrier, and the New Jersey Safety-Shaped barrier. A preliminary simulation, using the 820C Geo Metro model with the CalTrans Fluted Single Slope barrier shown in Fig. 9 (White et al. 2002) showed poor correlation with test results and raised concern regarding the validity of the vehicle model for use in this study.

The Fluted Single Slope barrier was angled 9.1 degrees from vertical with an overall height of the barrier was 1.42 m. The surface of the barrier was modified to incorporate flutes or ribs. The flutes were oriented at a 45° angle from the ground rising in the direction of vehicle travel. Each flute was 19 mm high and 19 mm wide. The flutes were spaced 50.8 mm on center along the length of the barrier. A 1990 Geo Metro impacted the barrier at a speed of 100 km/h and at an angle of 20°, as specified in NCHRP *Report 350*. The vehicle rolled over as it exited the barrier.

FIG. 9. CalTrans Single Slope Barrier with Fluted Surface Texture (White et al. 2002)

Simulation of the crash event did not produce vehicle climb nor rollover. The lack of vehicle climb and rollover in the simulation was attributed to rigid vehicle suspension components. The suspension elements could not replicate the overall vehicle behavior of the crash test with an absence of deformation and failure in the suspension components. Several changes to the 820C vehicle model were tried, but none improved the accuracy of the simulated vehicle performance on the three crash test systems. Consequently, the use of the 820C vehicle model in this study had to be abandoned.

3.3 2000P VEHICLE VALIDATION

To validate the NCAC Detailed 2000P Pickup Truck model, a comparison between crash test data and simulation results for the smooth Single Slope and New Jersey Safety-Shape barriers were performed. The crash test results for the Single Slope barrier were performed by TTI (Mak and Menges 1996). The Single Slope barrier, originally developed by TTI, was governed by NCHRP *Report 230* (Beason et al. 1989). The crash tests used in this report were to determine if the Single Slope barrier met the new NCHRP *Report 350* criteria. Shown in Fig. 10, is the simulation of the 2000P pickup truck with the smooth Single Slope barrier. Figures 11 through 13 illustrate the comparison of the crash test data to simulation results of vehicle roll, pitch, and yaw, respectively, for the Single Slope barrier. Each of these comparisons showed reasonable correlation, suggesting validity of the vehicle model on the Single Slope barrier.

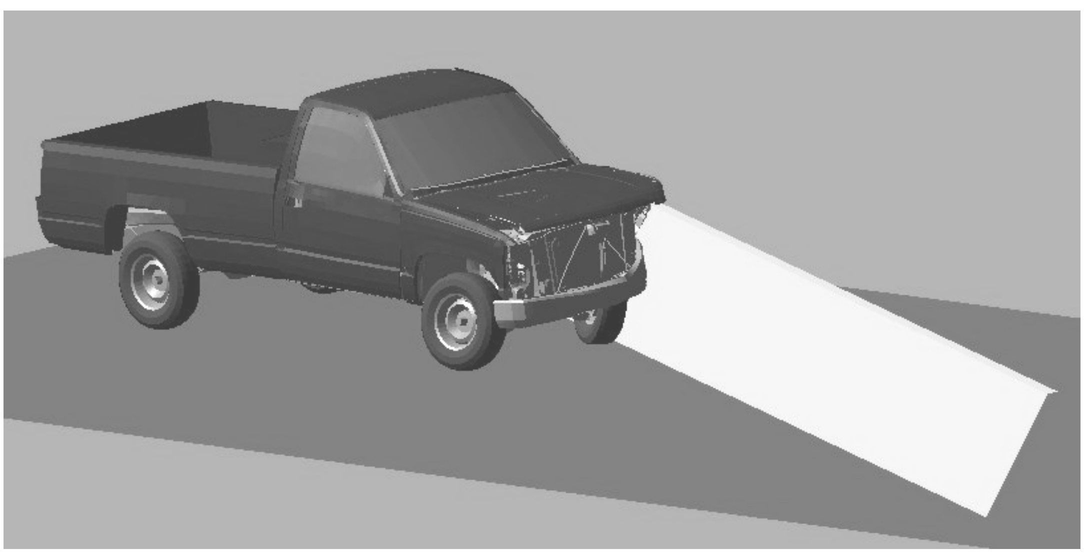

FIG. 10. Simulation of 2000P with Single Slope Barrier

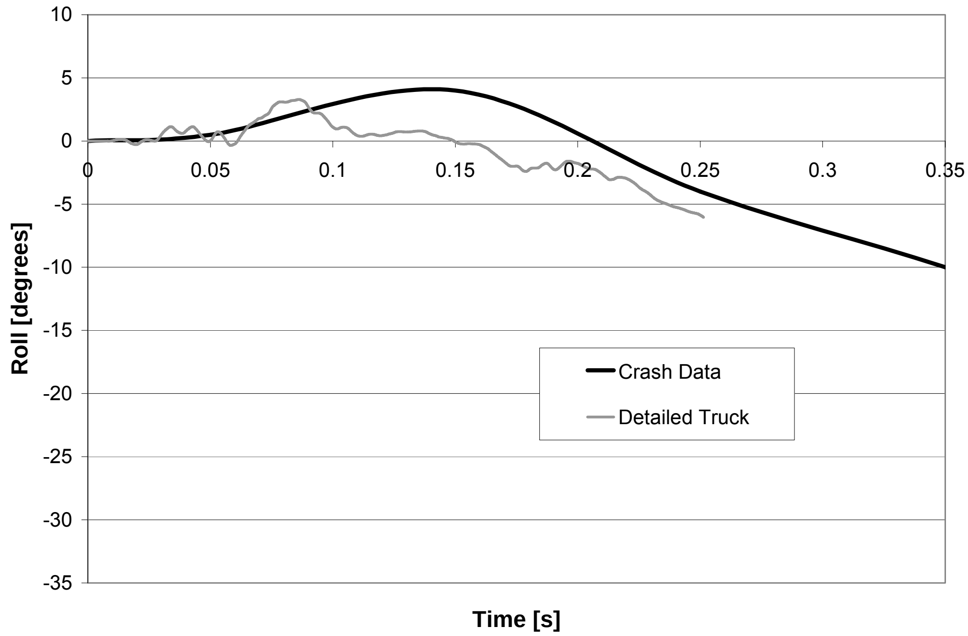

FIG. 11. Comparison of Roll Angles of Crash Data with Detailed Pickup Truck Vehicle Simulation on the Single Slope Barrier

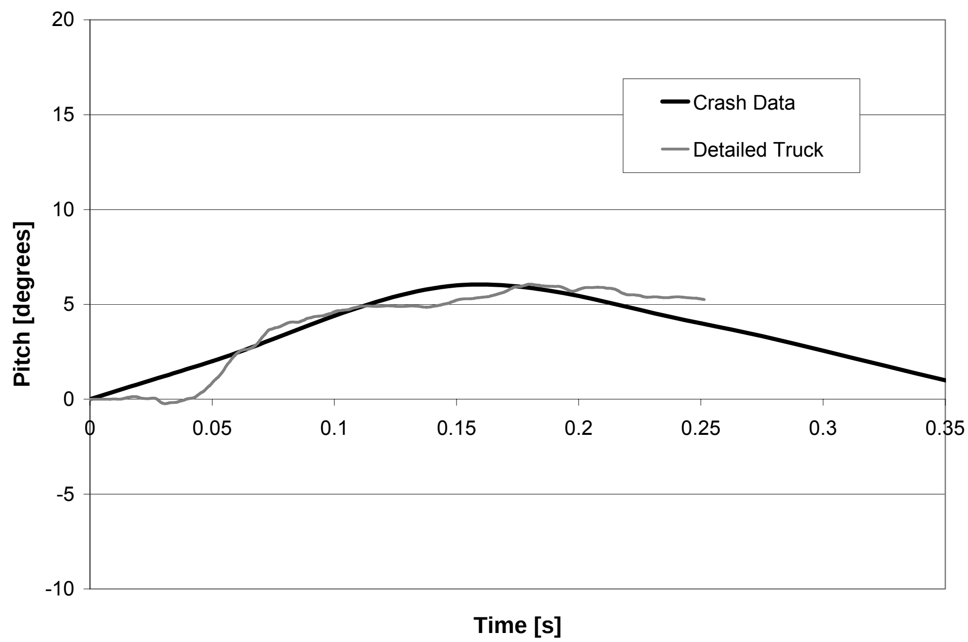

FIG. 12. Comparison of Pitch Angles of Crash Data with Detailed Pickup Truck Vehicle Simulation on the Single Slope Barrier

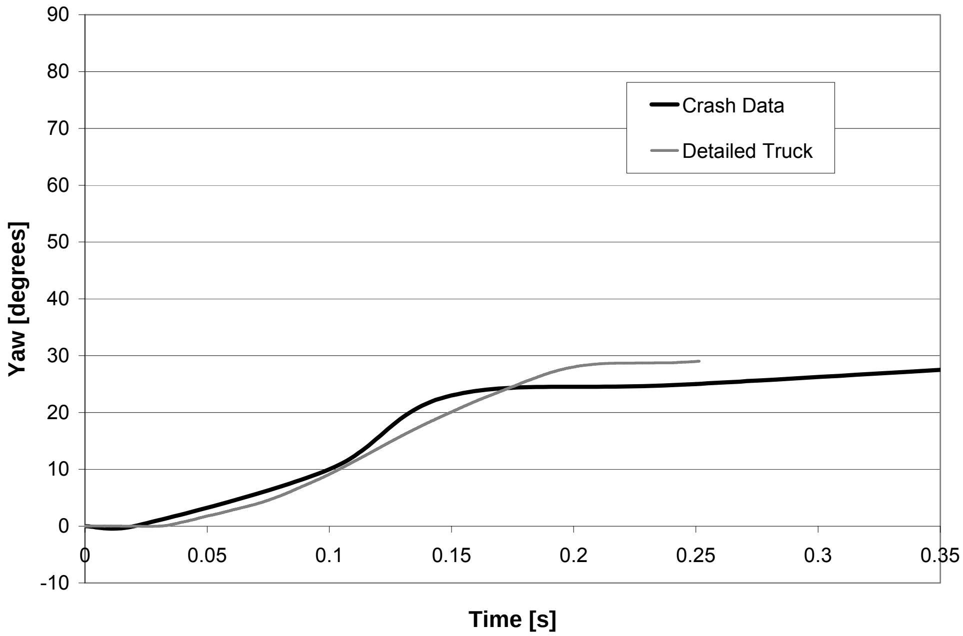

FIG. 13. Comparison of Yaw Angles of Crash Data with Detailed Pickup Truck Vehicle Simulation on the Single Slope Barrier

The New Jersey Safety-Shaped barrier crash test results used for comparison were performed by TTI (Buth et al. 1997a). These crash tests were done to evaluate several existing bridge rails under the new NCHRP *Report 350*. Fig. 14 shows the simulation of the 2000P pickup truck model with the New Jersey Safety-Shaped Barrier. Figures 15 through 17 show the comparison of the crash test data to simulation results of vehicle roll, pitch, and yaw, respectively, for the New Jersey Safety-Shape barrier. As with the Single Slope barrier, each of these comparisons also showed reasonable correlation, suggesting validity of the vehicle model on the New Jersey Safety-Shape barrier.

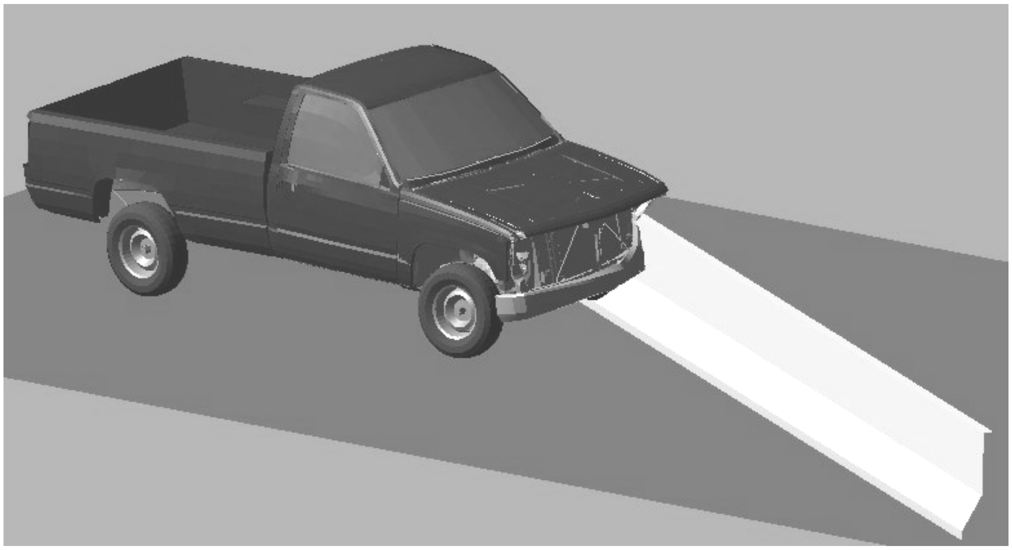

FIG. 14. Simulation of 2000P with New Jersey Safety-Shaped Barrier

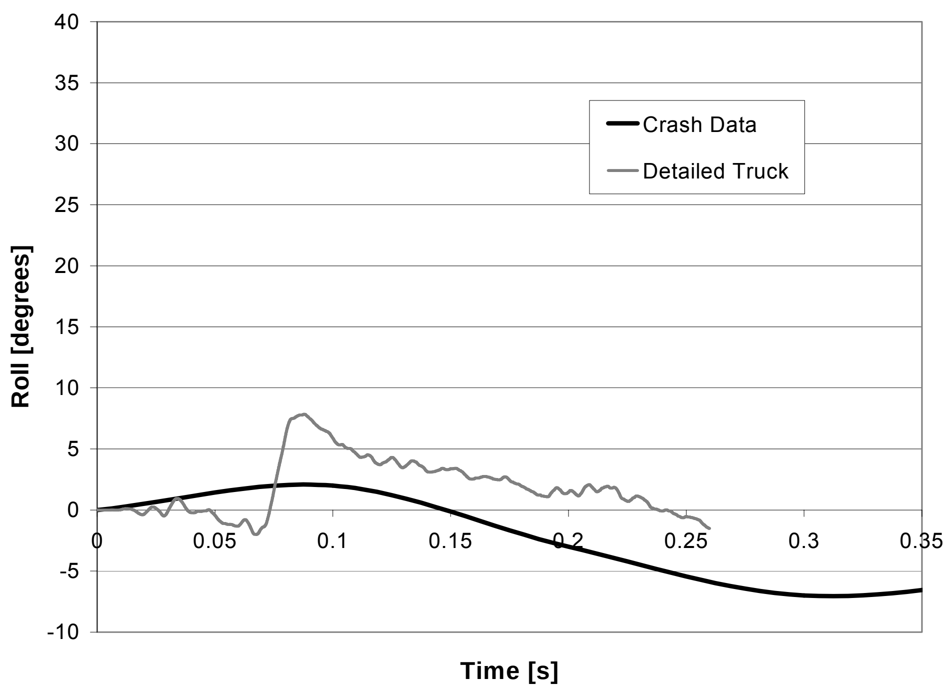

FIG. 15. Comparison of Roll Angles of Crash Data with Detailed Pickup Truck Vehicle Simulation on the New Jersey Safety-Shaped Barrier

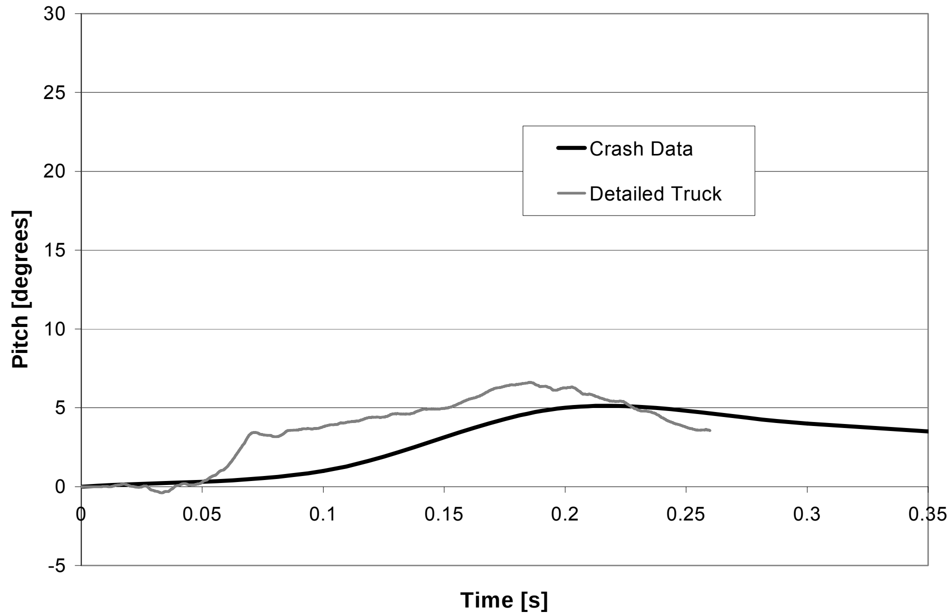

FIG. 16. Comparison of Pitch Angles of Crash Data with Detailed Pickup Truck Vehicle Simulation on the New Jersey Safety-Shaped Barrier

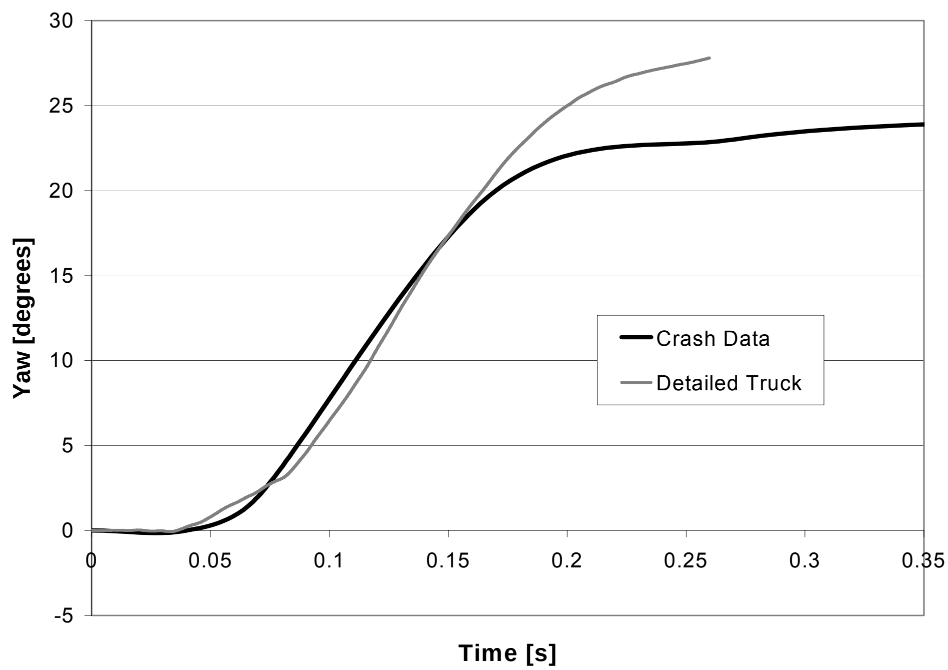

FIG. 17. Comparison of Yaw Angles of Crash Data with Detailed Pickup Truck Vehicle Simulation on the New Jersey Safety-Shaped Barrier

3.4 SUMMARY

Simulations with the 820C small car model clearly showed unrealistic vehicular response. Consequently, the interaction of the small car vehicle with barrier having surface asperities is not addressed in this study. Until significant improvements are made to the suspension of the 820C small car model, the ability to capture reasonable vehicle dynamics on barriers such as the Fluted Single Slope barrier will not be possible. The 2000P pickup truck model was validated for use in this project. A comparison of vehicle dynamics between the crash tests of the Single Slope barrier and New Jersey Safety-Shaped barrier were made to their corresponding simulations to validate the 2000P vehicle model.

4. SURROGATE MEASURE OF OCCUPANT COMPARTMENT DEFORMATION

4.1 OVERVIEW

OCD failure by NCHRP *Report 350* is excessive deformation of the occupant compartment that would cause severe harm to the occupant. Excessive OCD is a common cause of a failure in concrete barrier crash tests. As an example, excessive OCD failure was the most predominant type of failure in the CalTrans study “Crash Testing of Various Textured Barriers” (White et al. 2002). Fig. 18 illustrates occupant compartment deformation in a 2000P pickup truck after impact with a barrier. The NCAC 2000P Detailed Pickup Truck model has a good level of detail in the FEA representation, raising the possibility that the final deformed shape of the occupant compartment coming from simulation could be examined to extract an OCD value. This approach was explored, and found to be unsatisfactory for the reasons explained in subsequent sections of this section. Study of available crash tests and simulations of those crashes has lead to development of a suitable surrogate measure of OCD, which could

FIG. 18. Occupant Compartment Deformation (White et al. 2002)

be extracted from simulation results. The development of this surrogate measure is presented in this section.

4.2 POTENTIAL OCD SURROGATES

Several crash tests of concrete barriers with the 2000P pickup truck were available for study. However, the number of useful crash tests was limited because OCD was not measured nor reported in crash tests performed prior to the publication and adoption of NCHRP *Report 350*. A total of seven crash tests were found, which reported at least some information on OCD. Each of these crash tests were simulated using LS-DYNA. The details of those crash tests and their respective simulations are described in the next section. Each simulation was set up to collect several potential surrogate measures of OCD. A surrogate measure is a quantitative parameter, which can be evaluated in place of another parameter such as OCD that cannot be measured with adequate consistency. The surrogate measure that showed the best correlation with maximum OCD reported in the crash tests was selected.

The 2000P pickup truck model's deformation of the occupant compartment varies from simulation to simulation because the model does not accurately capture failure in the suspension. Without accurate failure of the suspension, the simulation did not replicate the correct load path. Some of the push back of the front wheel into the floorboard was restricted by connections to the suspension. A more general surrogate measure of OCD, which was not effected by load path, was needed. Even if the correct load path was not captured this methodology would be valid, as long as the surrogate measure showed adequate correlation to maximum OCD. Surrogate measure methodology has not been previously used in the field of roadside safety engineering.

The first potential surrogate measure of OCD was to make a direct measurement of the maximum deformation to the floorboard and toe pan of the vehicle model in a manner similar to that used in crash tests. The next potential surrogate measure of OCD was based on contact forces measured by LS-DYNA. An option was placed into the model to collect the direct impact forces between the wheel and barrier. These forces were evaluated using several criteria. The XY and XYZ resultants of the peak force, peak 10 ms moving average force, impulse over the time of initial impact, and total impulse were all computed and compared as an attempt of finding a correlation to OCD. XY and XYZ force resultants are the square root of the sum of the squares of each force component in the global coordinate system. The XY force resultant was used to remove the influence of the vertical component of the force on the data, which was not attributed to the pushing of the wheel assembly into the occupant compartment. The final potential surrogate measure of OCD was the internal energies of all of the parts in the crushing region of the vehicle, which were measured and checked for correlation to OCD. The internal energy in a part was related to the overall deformation undergone by that part.

4.3 AVAILABLE CRASH TEST DATA

Several crash tests were simulated to explore potential parameters for surrogate measure of OCD. All crash tests were concrete bridge rails or median barriers. In each of these crash tests, the test outcome was noted as either passing or failing and measured maximum OCD was reported in most cases. The surrogate measure of OCD was the parameter with the best correlation between maximum OCD and the measured value of each potential surrogate measures.

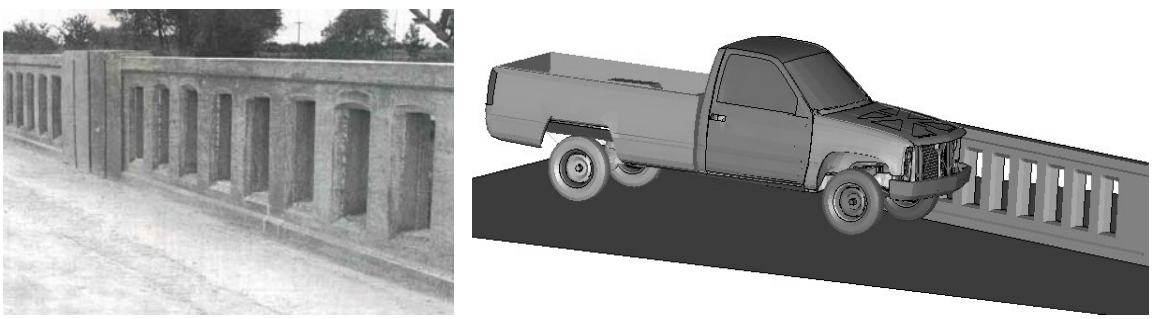

(a) (b)

FIG. 19. Oregon Bridge Railing: (a) Actual (Buth et al. 1997b); (b) Simulation

4.3.1 Oregon Bridge Railing

The Oregon Bridge Rail is a concrete beam and post bridge railing developed to give some see through making it more aesthetic. When the impact performance of this barrier was evaluated with the 2000P pickup truck, the OCD significantly exceeded the 150 mm limit imposed by FHWA (Buth et al. 1997b). Therefore, this test served as one of the failure points in the surrogate measure OCD study. Due to the pickup truck frame unrealistically snagging on the windows of this system and changing the vehicle dynamics, this data point was held in question.

Fig. 19 shows an image of the rail constructed for the crash test and the associated LS-DYNA model used in the simulation of the system.

4.3.2 Deep Cobblestone Barrier

The Deep Cobblestone barrier (shown in Fig. 20) is a random cobblestone surface treatment of a Single Slope barrier tested by CalTrans (White et al. 2002). The pickup truck test of this barrier failed due to excessive OCD caused by the interaction of the wheel and the large recesses between the cobblestones. The maximum depth of relief on the cobblestone surface is 64 mm. The cobblestone surface was modeled using hemispherical and ellipsoidal shapes with the same depth and spacing as the actual surface treatment. Because this was one of the few pickup truck crash tests with a solid concrete barrier that failed due to excessive OCD, it provides a useful data point for correlation of the surrogate OCD measures.

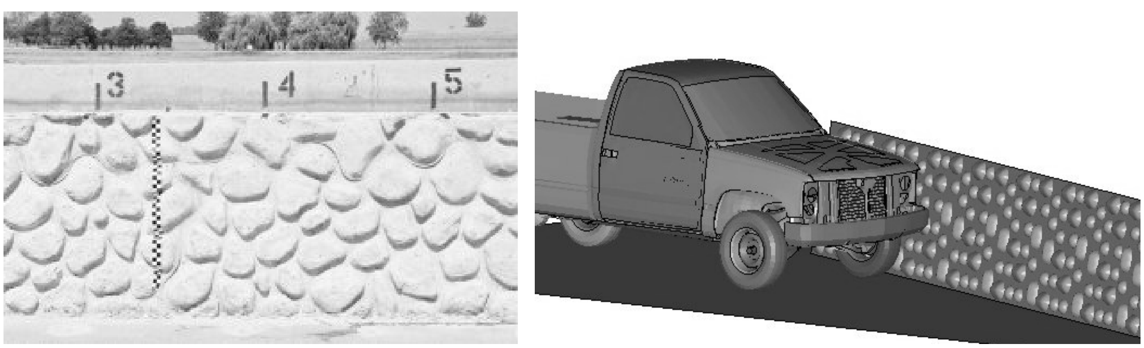

(a) (b)

FIG. 20. Deep Cobblestone Barrier: (a) Actual (White et al. 2002); (b) Simulation

4.3.3 Shallow Cobblestone Barrier

After the failure of the Deep Cobblestone barrier, the depth of the cobblestone surface treatment was reduced from 34 mm to 19 mm and retested (White et al. 2002). Typical relief of the Shallow Cobblestone barrier surface and the simulation setup is shown in Fig. 21. In the pickup truck crash test of this barrier, the drive shaft became dislodged from the transmission. Although the vehicle remained upright during the test, this type of damage was considered by

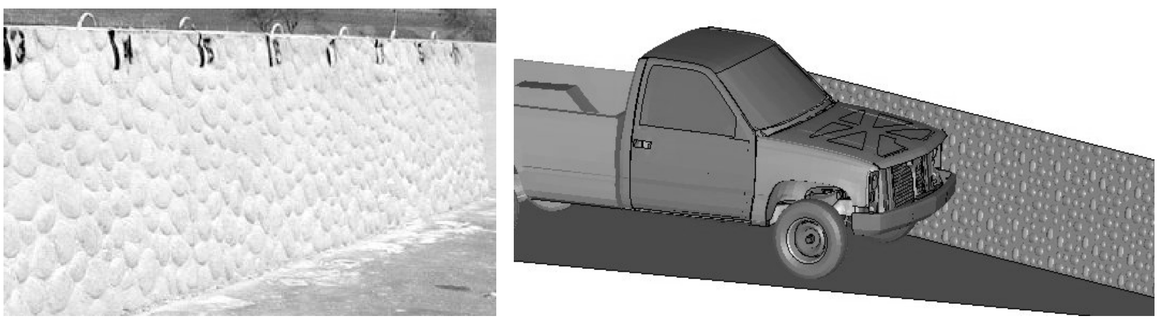

(a) (b)

FIG. 21. Shallow Cobblestone Barrier: (a) Actual (White et al. 2002); (b) Simulation

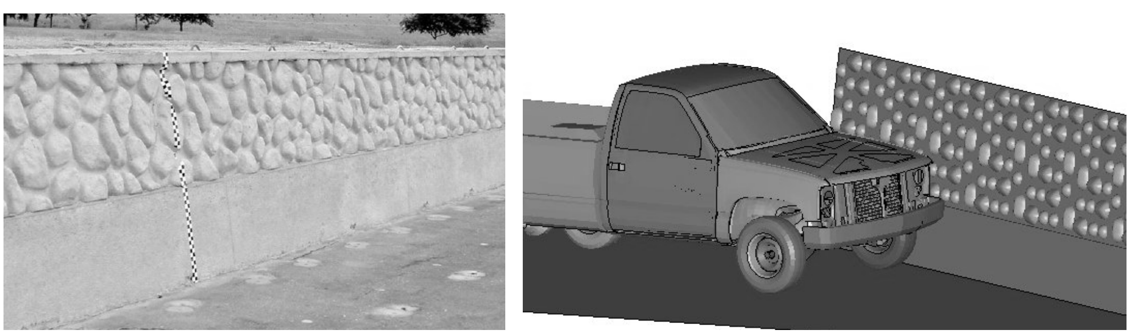

(a) (b)

FIG. 22. Cobblestone Reveal Barrier: (a) Actual (White et al. 2002); (b) Simulation

CalTrans to represent a potential rollover risk. As a result, CalTrans decided the barrier did not meet NCHRP *Report 350* evaluation criteria. However, since the shallow cobble reduced the maximum OCD of the vehicle to within acceptable limits, this test effectively illustrates the effect of surface asperity depth vehicle response, and represents another useful data point for purposes developing a surrogate measure for OCD.

4.3.4 Cobblestone Reveal Barrier

An alternative treatment developed to address the OCD problems associated with the Deep Cobblestone barrier was to provide a smooth reveal at the bottom of the barrier. The 610 mm tall reveal, which has a smooth sand blasted finish (see Fig. 22), is intended to reduce the snagging contact between the barrier and wheel assembly and, thereby, reduce the resulting OCD. This test successfully passed NCHRP *Report 350* criteria and provided another point for use in establishing the thresholds for a surrogate OCD measure. This barrier also possessed some similarity to the safety-shaped barriers that were addressed in this study, since the surface asperities were applied to the upper wall portion of the safety-shaped barrier while the toe of the barrier was left smooth.

4.3.5 Modified Texas T202

The Modified Texas Type T202 is a concrete beam-and-post system that has a vertical

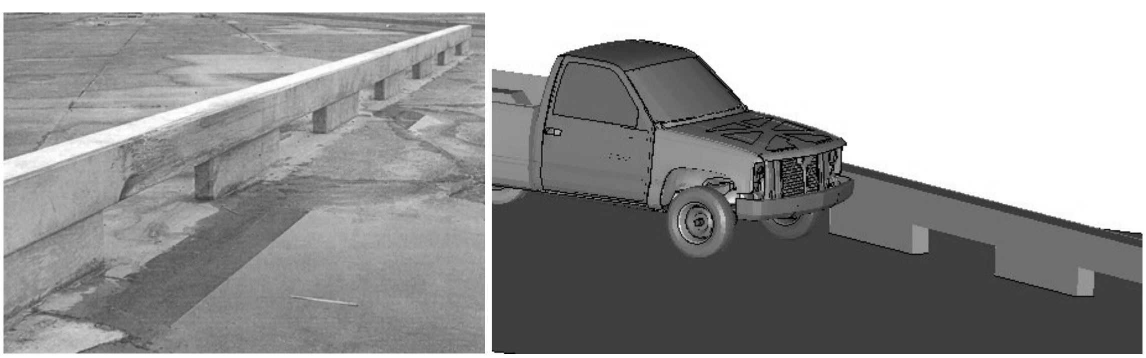

(a) (b)

FIG. 23. Modified Texas T202 Barrier: (a) Actual (Buth et al. 1998b); (b) Simulation

clear opening of 330 mm and a post setback of 114 mm. The Modified Texas Type T202 system and the simulation setup are shown in Fig. 23. Crash testing of this system was done by TTI (Buth et al. 1998b). The 2000P pickup truck passed NCHRP *Report 350* standards for the system and was used as one of the passing data points for this study.

4.3.6 Single Slope Barrier and New Jersey Safety-Shaped Barrier

The Single Slope barrier and New Jersey Safety-Shaped barrier systems were modeled and evaluated was part of the surrogate measure of OCD study. Each of these tests had acceptable OCD, which is less than 150 mm and met NCHRP *Report 350* guidelines. These passing crash tests provide confidence in establishing a passing threshold for the selected surrogate OCD criterion.

4.4 COMPARISON OF OCD AND POTENTIAL SURROGATES FOR AVAILABLE CRASH TESTS

Direct measurements of OCD were obtained from the simulations and compared to measured full-scale crash test OCD values. As shown in Fig. 24, induced buckling, resulting from compression of the floorboard, could overstate the maximum OCD due to localized effects. In an actual crash test, direct contact from the wheel, wheel well, fender, and other parts may contact the floorboard and cause additional OCD. Although the overall deformation remained proportional between test and simulation, the usefulness of direct measurements was questioned. As shown in Table 1, there was some correlation observed between the simulation

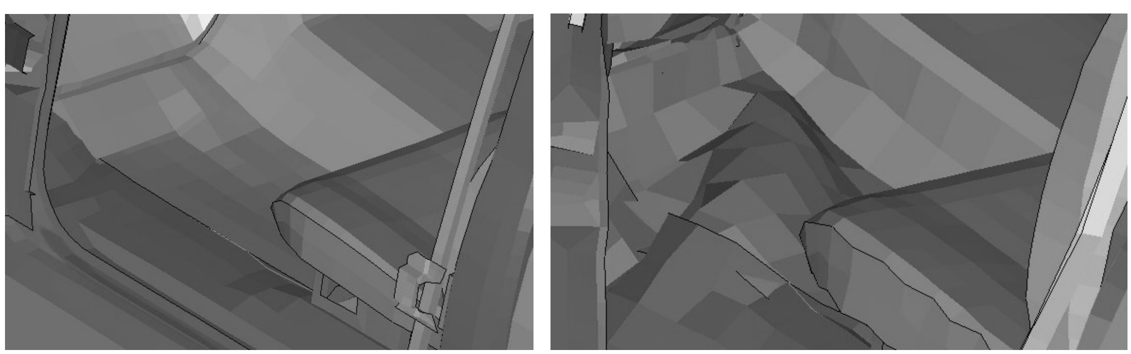

(a) (b)

FIG. 24. Truck Model Buckling Floorboard: (a) Undeformed; (b) Deformed

and test data. Since these results were highly influenced by localized buckling, direct measurement of OCD was not selected as the surrogate measure of OCD.

Simulation contact forces between the wheel and the barrier have been tabulated in Table 2. Force data was evaluated using the process as discussed in the previous section. Crash test OCD data was compared to each of the measures from the simulation. Poor correlation was found using these measures. This was possibly due to the unreliable values of force between parts undergoing such severe deformation. The amount of separation or range that exists in this data between acceptable and failed crash tests was not adequate to permit these measures to be confidently used as a surrogate measure for OCD.

The most conclusive internal energy results from all of the parts evaluated in the crush region of the pickup truck model were the floorboard and wheel well parts. The comparison of these internal energy results to crash test maximum OCD values can be seen in Table 3. Internal energies obtained from the floorboard and wheel well showed the best correlation to the actual crash test results among the measures evaluated. Therefore, these parts were selected for further study in the search for a surrogate measure of OCD.

Internal energy is the same thing as strain energy, which is computed as one half of the product of stress and strain integrated over the element (1998). Therefore, internal energy and overall deformation undergone by an element are directly proportional. Collecting the internal energy data from LS-DYNA was done by taking the final internal energy output from the database file created to monitor the energies of each part of the simulation. The internal energy was outputted as a cumulative quantity for each part over the time of the simulation. Between the floorboard and wheel well, the floorboard was selected as the surrogate measure of OCD. Even though the wheel well showed slightly better correlation, the floorboard was chosen because it was less influenced by differences in load path and did not experience as large of deformations as the wheel well.

Table 1. Direct Measurements for Truck OCD Study

Name	Pass / Fail	Crash Test OCD [mm]	Direct Measurement [mm]
Oregon	Fail	475	170
Cobblestone	Fail	160	225
Cobblestone with Reveal	Pass	98	50
Single Slope	Pass	140	50
New Jersey	Pass	Not Reported	80
Modified T202	Pass	130	80
Shallow Cobble	Pass	133	105

Table 2. Wheel to Barrier Contact Forces and Impulses for Truck OCD Study

			X-Y-Z Resultant			
Name	Pass / Fail	Crash Test OCD [mm]	Max Force [N]	Max 10 ms Moving Avg. [N]	Impulse [N-s]	Total Impulse [N-s]
Oregon	Fail	475	1,290,000	459,000	28,800	29,900
Cobblestone	Fail	160	1,340,000	450,000	34,500	40,100
Cobblestone with Reveal	Pass	98	278,000	195,000	14,500	14,800
Single Slope	Pass	140	510,000	164,000	10,700	15,200
New Jersey	Pass	Not Reported	229,000	197,000	12,100	12,800
Modified T202	Pass	130	290,000	231,000	12,800	21,100
Shallow Cobble	Pass	133	910,000	459,000	18,700	18,700
			X-Y Resultant			
Oregon	Fail	475	1,290,000	455,000	27,700	28,300
Cobblestone	Fail	160	1,176,000	438,000	31,900	35,900
Cobblestone with Reveal	Pass	98	276,000	195,000	14,300	14,600
Single Slope	Pass	140	498,000	164,000	10,600	15,100
New Jersey	Pass	Not Reported	228,000	196,000	12,000	12,700
Modified T202	Pass	130	263,000	123,000	11,900	19,800
Shallow Cobble	Pass	133	901,000	449,000	18,000	18,000

Table 3. Internal Energies for Truck OCD Study

Name	Pass / Fail	Crash Test OCD [mm]	Floorboard Part (73) [N-mm]	Wheel Well Part (54) [N-mm]
Oregon	Fail	475	9,826,000	14,140,000
Cobblestone	Fail	160	10,783,000	11,040,000
Cobblestone with Reveal	Pass	98	782,400	3,980,000
Single Slope	Pass	140	721,300	2,469,000
New Jersey	Pass	Not Reported	1,130,000	2,870,000
Modified T202	Pass	130	1,172,000	3,300,000
Shallow Cobble	Pass	133	2,150,000	7,540,000

4.5 SELECTED SURROGATE MEASURE OF OCD

The internal energy of the floorboard of the NCAC 2000P Detailed Pickup Truck model was selected as the most appropriate surrogate measure for evaluating OCD. This is a measure of the overall deformation done to this part. Using the internal energy from the simulations and the reported OCD values from the crash tests, thresholds for the surrogate measures were established. As shown in Fig. 25, the passing limit was selected as 2,200 N-m and the failure limit was set at 10,700 N-m of internal energy in the floorboard of the NCAC 2000P Detailed Pickup Truck model. These limits were selected as values of internal energy, which separate the definite passing and failing regions from the unknown or marginal region between them.

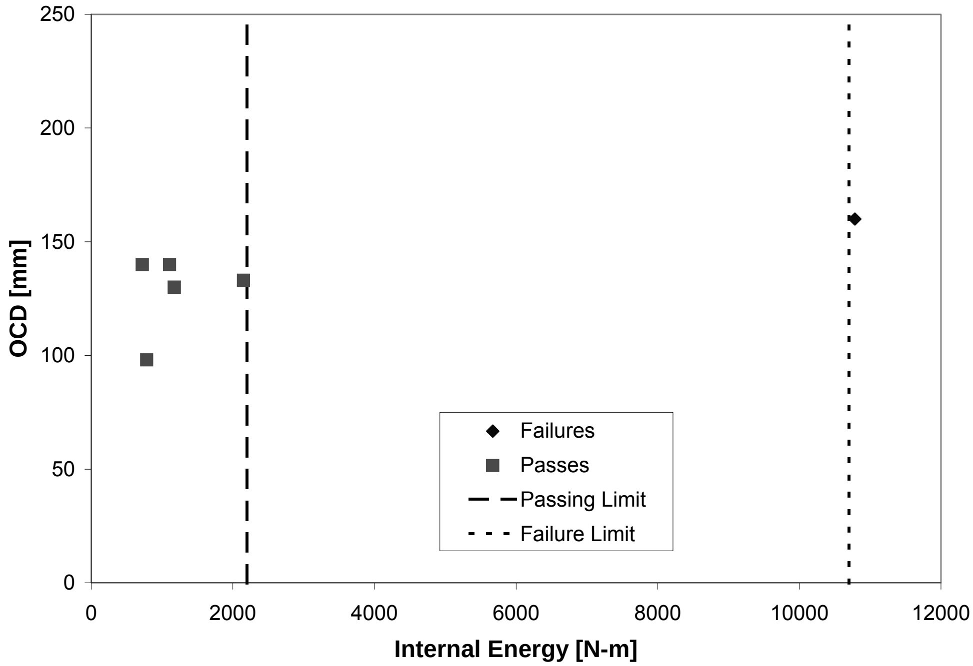

FIG. 25. Passing and Failing Crash Tests OCD vs. Internal Energies of Floorboard

The interaction of the vehicle with the Oregon Bridge Rail was considered to be substantially different than what typically occurs in an impact with a solid barrier. The frame rail of the pickup truck protruded inside one of the windows and snagged severely on the inside of one of the concrete posts. As a result, instead of the load going to the floorboard, as it does in most OCD failures, the load was directed to the frame. Therefore the Oregon Bridge Rail crash test was not taken into consideration when selecting the failure limit. The passing limit and failing limit have a large range of internal energies, but only a small difference in OCD. This causes some uncertainty in the value of the failure limit since it was based on a single failure data point.

5. PARAMETRIC STUDY

5.1 OVERVIEW

To develop guidelines for the aesthetic surface treatment of safety-shaped median barriers a parametric study was performed using simulated crash events. Each crash event was simulated with the NCAC 2000P Detailed Pickup Truck model impacting a rigid New Jersey Safety-Shaped barrier with surface asperities added to the upper face. As defined in the NCHRP *Report 350* for test level 3, the vehicle speed and angle of impact were 100 km/hr and 25°, respectively. Twenty nine simulated crashes were performed. Each crash had a slightly different barrier surface geometry. Each simulation was categorized as passing, marginal, or failing, based on the surrogate measure of OCD. This was done by measuring the internal energies in the floorboard of the 2000P pickup truck model and compared to the passing and failure limits of 2,200 N-m and 10,700 N-m, respectively.

Fig. 26 shows the location of the surface asperities on the New Jersey Safety-Shaped barrier. These asperities were actually created by depressing panels on the upper face of the barrier profile between each asperity. Therefore, the original barrier profile was unchanged along each of the asperities. A plan view of the barrier profile can be seen in Fig. 27. This figure illustrates the variables used in this parametric study, which are the width of recess "W", the depth of recess "d", and the angle of asperity "θ". The parametric study was performed with 45°

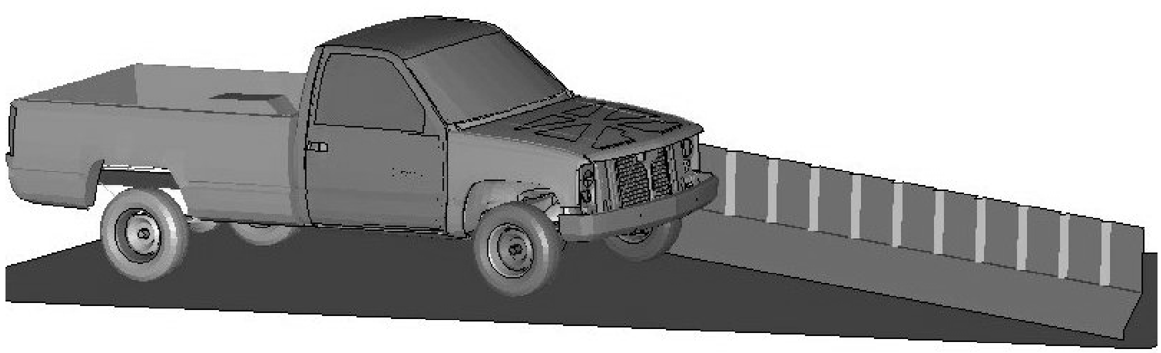

FIG. 26. Parametric Study Simulation Setup

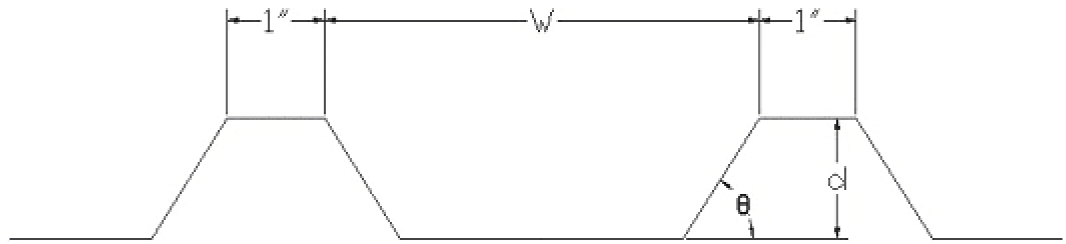

FIG. 27. Surface Asperities Geometry Variables

and 90° angles of asperities. While each of the angles of asperities were held constant, the depth and width of recess were varied.

Another interesting point about angled asperities is that when the angle is less than 90°, depth and width of the asperity are not always independent of one another. From Fig. 27 you can see that as the width "W" decreases, the surface asperities become closer together until the sloped sides of the asperities create a "V" shaped relief. Once "W" decreases beyond that point, the depth "d" must also decrease, since the angle of the asperities is held constant. Fig. 28 shows the geometric boundary for the angle of asperity equal to 45°. Only geometries that are within the cross hatched region are possible.

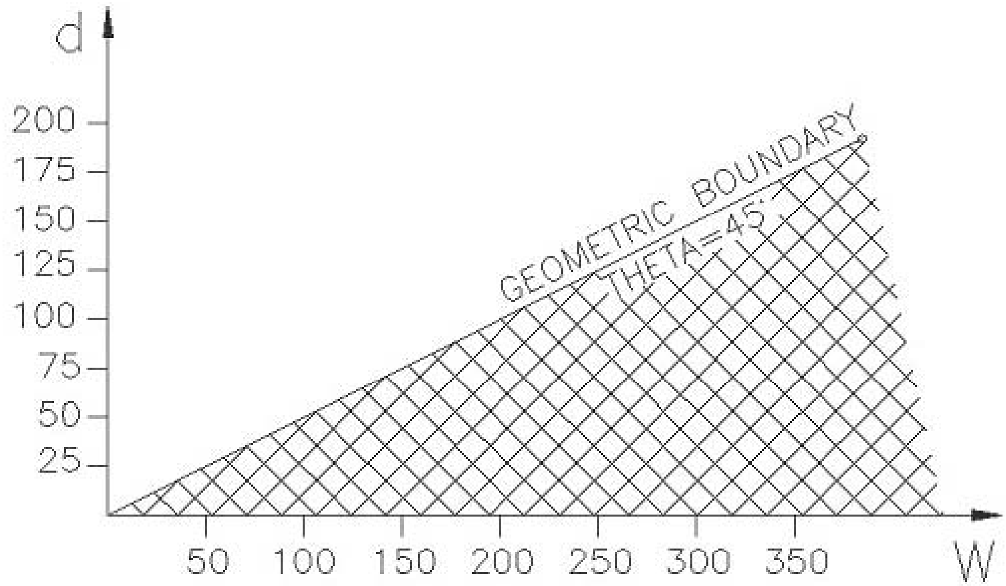

FIG. 28. 45° Geometric Boundary between Recess Depth and Width

A typical practice in simulation is to model a concrete barrier or bridge rail as shell elements with rigid material properties. By making the material rigid there are several advantages and disadvantages involved. A significant advantage to modeling the barrier as a rigid material was the reduction in simulation time needed by LS-DYNA to process these elements. A disadvantage was the concrete was not able to spall or chip off as expected in most of these crash test setups. Without the model's ability to capture the expected concrete spalling, the guidelines developed by this research are conservative in nature.

5.2 SIMULATION RESULTS AND FINDINGS

In the previous section the system setup and variables of the parametric study were discussed. Simulation results for the 45° angle of asperities are presented in Table 4. Each simulation compared the internal energy of the floor board to the passing and failing limits, established in the previous section, to determine if the simulation had passing, marginal, or failing OCD. Simulations with zero depth refer to the same smooth New Jersey Safety-Shaped barrier simulation, and were included to illustrate the trend of the floor board internal energy as the depth goes to zero for each width. The remaining simulated geometries were selected by holding angle "θ" and width "W" of the asperity constant while changing the depth *d* of the asperity. The depth was decreased from a failing OCD to zero depth. For all simulated values of “W” and “θ”, a curve passing between the data points of marginal and failed configurations was plotted as shown in Fig. 29.

Table 4. Parametric Study Results for 45° Angle of Asperity

Run #	Vehicle	Asperity Width (W) [mm]	Asperity Depth (d) [mm]	Truck Floorboard Internal Energy [N-m]	Pass/Fail
1	Truck	555	100	18,318	Fail
2	Truck	555	75	15,939	Fail
3	Truck	555	62.5	12,835	Fail
4	Truck	555	50	8,397	Marginal
5	Truck	555	37.5	6,986	Marginal
6	Truck	555	25	4,341	Marginal
7	Truck	555	12.5	2,422	Marginal
8	Truck	555	0	1,108	Pass
9	Truck	280	62.5	15,507	Fail
10	Truck	280	37.5	14,680	Fail
11	Truck	280	25	8,965	Marginal
12	Truck	280	12.5	3,038	Marginal
13	Truck	280	0	1,108	Pass
14	Truck	180	25	11,844	Fail
15	Truck	180	12.5	4,905	Marginal
16	Truck	180	0	1,108	Pass
17	Truck	80	25	17,182	Fail
18	Truck	80	12.5	7,391	Marginal
19	Truck	80	0	1,108	Pass
20	Truck	30	15	4,149	Marginal

Passing Limit=2,200 N-m
Failure Limit=10,700 N-m

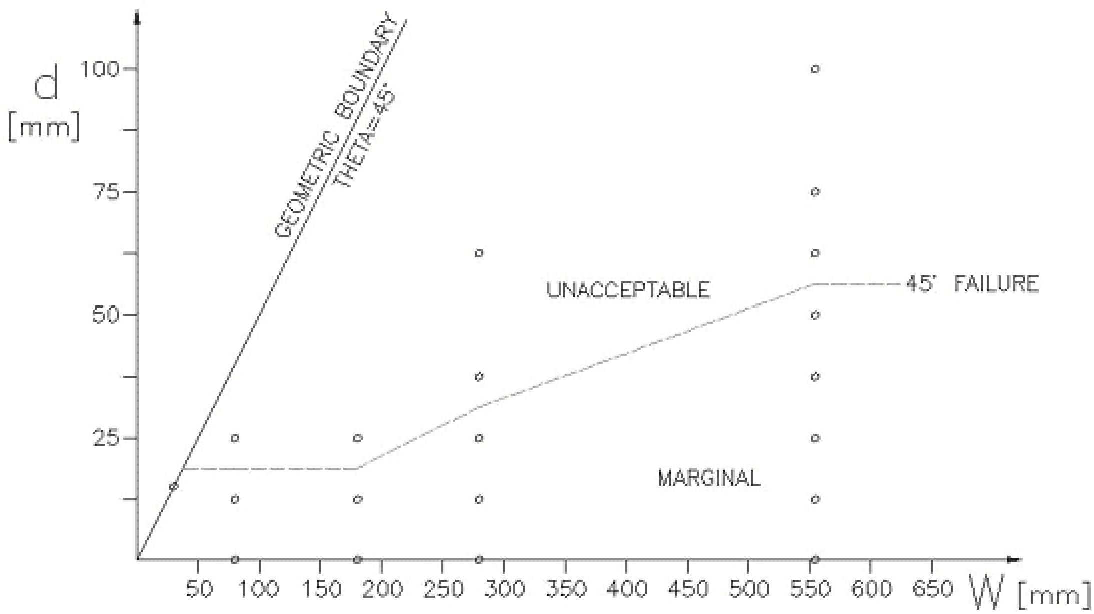

FIG. 29. Depth vs. Width Parametric Results for a 45° Angle of Asperity

The addition of any surface asperities caused the surrogate measure to predict only marginal or failed OCD as a result. Therefore, the failure line has been shown on the guideline, but the passing line is not shown because it exists along zero depth.

Similar results for the 90° angle of asperities are presented in Table 5 and the curve is shown in Fig. 30. It can be seen from the simulation results that almost all of the simulations with asperity depth “d” equal to or greater than 12.5 mm were either marginal or failed the OCD evaluation criteria. It was likely that if the depth “d” is further reduced from 12.5 mm, some of the configurations may pass the OCD criteria. However, such small depths may be of little or no significance from the standpoint of aesthetic design guidelines for barriers and hence were not evaluated. The curves shown in Fig. 29 and Fig. 30 thus only show a failure line, above which, the configuration was predicted to fail the crash test and below which, the configuration was predicted to give a marginal or a possibly passed test.

Future crash testing will be needed for a passing curve to be added to the plots, or the failure curve can be adjusted, depending on whether the crash test passed or failed. If a marginal configuration is crash tested and passes NCHRP *Report 350* criteria, it would change the passing limit and hence a passing curve will be added to the plots. If, however, a marginal configuration being crash tested fails, the failure limit would change and the failure line will be adjusted accordingly.

Table 5. Parametric Study Results for 90° Angle of Asperity

Run #	Vehicle	Asperity Width (W) [mm]	Asperity Depth (d) [mm]	Truck Floorboard Internal Energy [N-m]	Pass/Fail
1	Truck	5	50	2,157	Pass
2	Truck	30	50	6,049	Marginal
3	Truck	30	25	6,077	Marginal
4	Truck	30	12.5	3,257	Marginal
5	Truck	30	0	1,108	Pass
6	Truck	55	50	25,000+	Fail
7	Truck	55	25	Error	Fail
8	Truck	55	12.5	17,497	Fail
9	Truck	55	0	1,108	Pass
10	Truck	280	25	30,000+	Fail
11	Truck	280	12.5	6,453	Marginal
12	Truck	280	0	1,108	Pass
13	Truck	580	37.5	14,000+	Fail
14	Truck	580	25	8,909	Marginal
15	Truck	580	12.5	3,506	Marginal
16	Truck	580	0	1,108	Pass

Passing Limit=2,200 N-m
Failure Limit=10,700 N-m

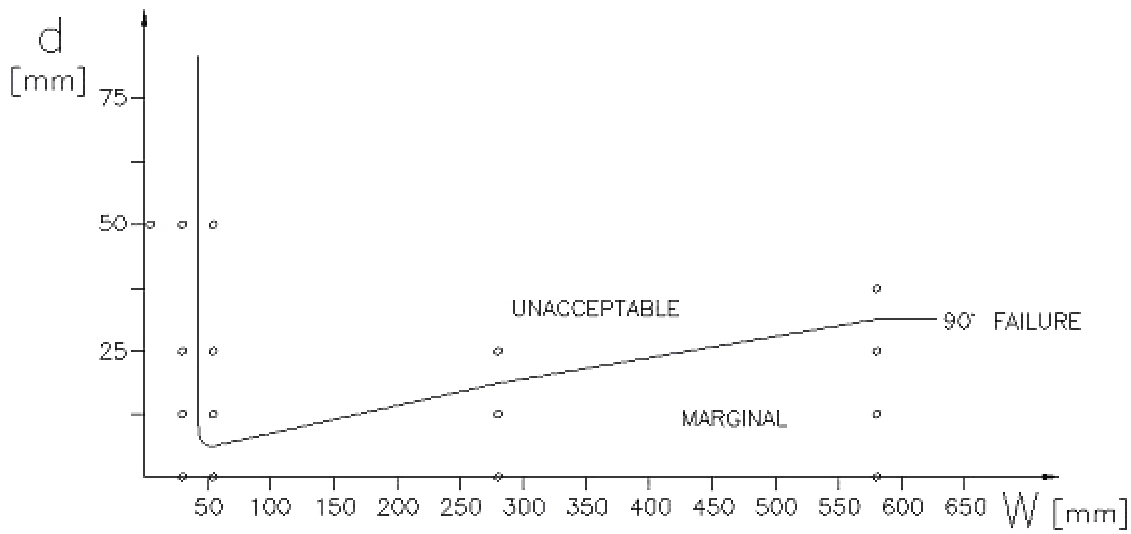

FIG. 30. Depth vs. Width Parametric Results for a 90° Angle of Asperity

As expected, Fig. 30 shows that the 90° angle of asperity curve limits the asperity depth more than the 45° angle of asperity. Also as expected, both 90° and 45° angles of asperity curves have similar shapes. It is also worth mentioning that given the curves for 90° and 45° angles of asperity, curves for intermediate angles of asperity can be developed by linearly interpolating the results.

Looking at the shape of the guideline curves for 45° and 90° angles of asperities, the effects of asperity width and depth on barrier performance were as expected. When the asperity width “W” is small, the vehicle’s impact path crosses more asperities. This in turn presents more resistance to vehicle sliding on the barrier and causes more damage to the vehicle. Consequently we see a reduction in the allowable asperity depth “d” for these smaller widths. As the width of asperity increases, the allowable depth “d” also increases. This increase in allowable depth “d” becomes a constant value when the vehicle’s impact path only crosses a single asperity or too few asperities.

6. SUMMARY AND CONCLUSIONS

6.1 OVERVIEW

The aim of this research was to develop guidelines for the aesthetic surface treatment of safety-shaped median barriers. This was done using numerical simulation of a parametric study, which varied surface geometry on the upper face of a New Jersey Safety-Shaped barrier. A 2000P pickup truck model was validated and a surrogate measure for OCD was found. By using the internal energy of the truck model floor board passing and failure limits were established for determining a passing, marginal, or failing OCD by NCHRP *Report 350* standards in the simulation. The parametric study varied width and depth between surface asperities for a given angle of asperity. Guidelines were developed from the results of this parametric study.

6.2 BARRIER SURFACE ASPERITY SELECTION

In this research, guidelines were developed for aesthetic surface treatment of safety-

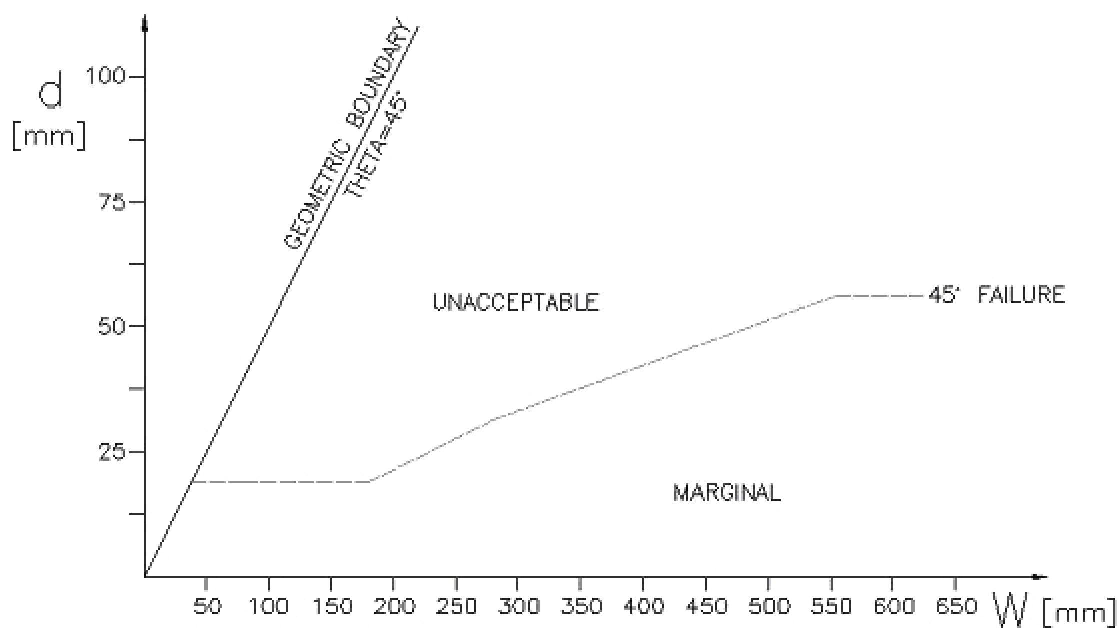

FIG. 31. Depth vs. Width Guideline for a 45° Angle of Asperity

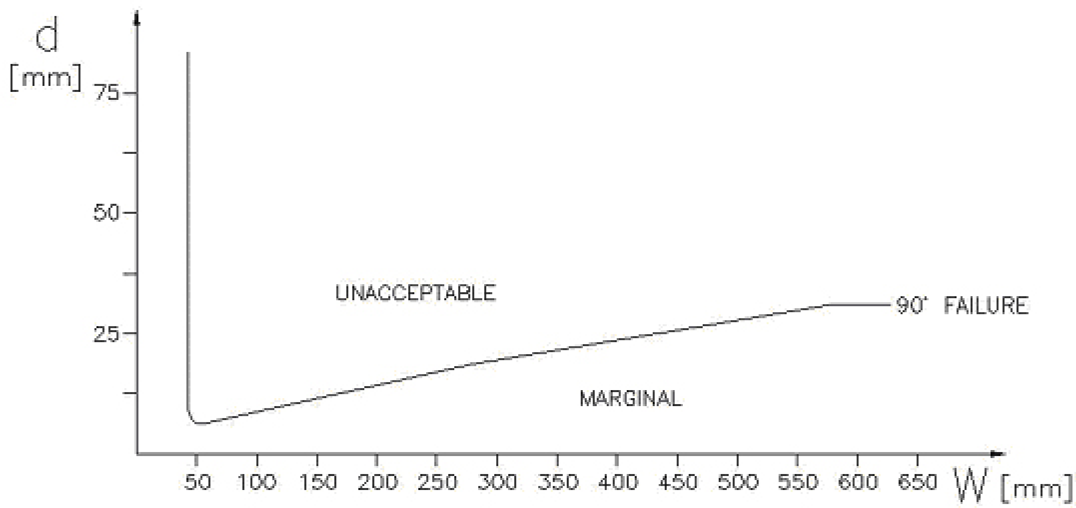

FIG. 32. Depth vs. Width Guideline for a 90° Angle of Asperity

shaped median barriers. Those guidelines are contained in Fig. 31 and 32, the guidelines were determined for the 45° and 90° angles of asperities as a curve on depth vs. width of asperity.

Using these guidelines, a designer can avoid a definite failure of their surface treatment by NCHRP *Report 350* standards. After crash testing is done to adjust and validate the curves bringing them to their final form, new surface treatments will not require full-scale crash testing, but only need to be within the acceptable region on these guidelines.

To use these guidelines a designer can approximate their surface geometry into terms of width of recess "W", the depth of recess "d", and the angle of asperity "θ". The guideline's recommendation is found by locating the region of the guidelines that their surface geometry is within. The unacceptable region predicts a definite failure of the surface geometry. The marginal region predicts a possible passing surface geometry. This marginal or unknown region was needed to capture the uncertainty of the guidelines in its present form. At this point in the guidelines development there was not an acceptable region above a safety-shaped barrier with no surface asperities. When an acceptable region is established this region will predict a definite pass of NCHRP *Report 350* standards.

6.3 LIMITATIONS AND CONCERNS

A significant limitation of this research is the absence of data for the 820C small car vehicle. This leaves the issue of the 820C small car's vehicle stability unanswered. This limitation can only be addressed once vehicle model improvements are made to the 820C small car vehicle model making it valid for use in research of this type. Limited crash test data was another limitation faced throughout this research.

Comparing the guidelines concluded from this research to the CalTrans existing guidelines for Single Slope barrier is difficult because CalTrans recommendations only include a restriction on asperity depth to 25 mm for asperities with 45° angle or less and 13 mm for asperities with 90° angle or less. The CalTrans recommendations are also only on a pass/fail basis without a marginal region and do not take spacing of the asperities into account. As expected the CalTrans recommendations were more restrictive on depth of asperity than the failure line on most widths of recess. Only for asperities with a 45° angle and a width of recess less than 250 mm was the depth of recess restricted more by the guideline established by this research.

During the course of the parametric study, it was found that a potential for door snagging with asperities on the barrier exists. This was more of a concern with the 90° asperities as compared to the 45° asperities. Since the door hinges and latches in the NCAC 2000P Detail Pickup Truck model were not modeled to capture this failure mode of the door, a detailed prediction with each asperity configuration cannot be made. Moreover, it should be noted that due to the lack of a robust concrete material model, the barriers were modeled with rigid material. One may expect to see some concrete failure in the asperities during the actual crash test, which in fact would reduce the overall vehicle damage and door snagging problem for some configurations. However, the potential for this snagging still exist and is difficult to quantify thru simulation due the limitations previously mentioned. Previous research has shown that small asperity depths with close to a 90° asperity angle can cause significant damage to the vehicle and consequently fail the test (Bullard et al. 2002). Most of these cases involve snagging due to an exposed edge of a rail splice or a bridge rail transition. Even though the exposed edge has a very small thickness (asperity depth), the sharp angle of about 90° with respect to the vehicle travel path (asperity angle) causes a significant damage to the vehicle (Buth et al. 2000, Buth et al. 1999, and Buth et al. 1993).

Another concern was that none of the simulations of the parametric study predicted a definite passing OCD beyond a width of 5 mm. Even though these guidelines are conservative in nature at this point it could be concluded that adding any kind of a surface treatment to a safety-shaped barrier is not highly recommended.

6.4 FUTURE RESEARCH

The next step in finalizing these curves is to crash test several different surface geometries. The geometries selected will be from the marginal region of the guidelines. If a marginal configuration being crash tested passes the NCHRP *Report 350* criteria, it implies that any asperity depth less than the one tested would also pass. Hence this would lead to adding a passing curve to the plots. However, if a marginal configuration being crash tested fails, this would imply that any asperity depth higher than the one tested would also fail. Hence the failure line will be adjusted accordingly. This adjustment after the crash testing phase will lead to the final design guidelines.

As with most research more questions than answers have been found by our work on this topic. Several issues have been found that could be researched further. Finding an equivalent angle of asperity for a rounded asperity would be needed for designers working with rounded components in their aesthetic surface treatment. One of the crash tests mentioned in this research was the Cobblestone Reveal barrier, which removed the surface treatment from a lower section of the barrier. The Cobblestone barrier with the same surface treatment all the way to the ground had failed due to OCD. Therefore, the removal of the surface treatment had made the OCD acceptable. With the lower section of the surface treatment removed, designers would get more depth to work with in their designs.

Beyond this project further research into creating more accurate and reliable vehicle models is needed. When the vehicle models were first developed their purpose was to give a generally accurate crush stiffness to be able to measure roadside system performance or global parameters such as vehicle dynamics. As research continues to focus more heavily on vehicle deformations of individual components the connections between these components will need to be improved. Many phenomena that are faced in the area of roadside safety are highly dependent on failure of connections and joints in the vehicle model. At this time, LS-DYNA is releasing versions that can define failure in connections and joints, but to determine acceptable values to set to these parameters can be very difficult. Many roadside safety systems have been influenced greatly by rim interaction with the system presenting a need for a tire model with the ability to fail and air out. Until the tire failure can be modeled, the rim interaction with the system can not be captured.

REFERENCES

American Association of State Highway and Transportation Officials (AASHTO). (1996). *Roadside Design Guide*, Washington, D.C.

Beason, W. L., Ross, H. E., Perera, H. S., Campise, W., and Bullard, D. L. (1989). "Development of a single slope concrete median barrier." *Report No. 9429CDK-1*, Texas Transportation Institute, Texas A&M University, College Station, Texas.

Bullard, D.L. Jr., Williams, W.F., Wanda, L.M., and Haug, R.R. (2002). "Design and evaluation of the TxDOT F411 and T77 Aesthetic Bridge Rails." Research *Report 4288-1*, Texas Transportation Institute, Texas A&M University, College Station, Texas.

Buth, C.E., Hirsch, T.J., and Wanda, L.M. (1993). "Testing of new bridge rail and transition designs, Volume XIII: Appendix L." Texas Transportation Institute, Texas A&M University, College Station, Texas.

Buth, C. E., Hirsch, T. J., and Menges, W. (1997a). "Testing of new bridge rail and transition designs, Volume VI: Appendix E 32-in (813-mm) New Jersey Safety Shape." *Report No. FHWA-RD-93-063*, Texas Transportation Institute, Texas A&M University, College Station, Texas.

Buth, C. E., Menges, W., and Butler, B. G. (1997b). "Testing and evaluation of NCHRP 350 test level four concrete bridge railing for Crooked River Gorge 18211." *Project No. 405890-1*, Texas Transportation Institute, Texas A&M University, College Station, Texas.

Buth, C. E., Bligh, R. P., and Menges, W. (1998a). "NCHRP Report 350 Test 3-11 of the Texas T411 Bridge Rail." *Report No. FHWA/TX-98/1804-3*, Texas Transportation Institute, Texas A&M University, College Station, Texas.

Buth, C.E., Williams, W.F., Bligh, R.P., Wanda, L.M., and Butler, B.G. (1998b). "NCHRP Report 350 testing of the Texas Type T202 Bridge Rail." *Report 1804-3*, Texas Transportation Institute, Texas A&M University, College Station, Texas.

Buth, C.E., Wanda, L.M., and Williams, W.F. (1999). "Testing and evaluation of the New York Two-Rail Curbless and Four-Rail Curbless Bridge Railing and the Box-Beam Transition." *FHWA Contract DTFH61-98-C-00056*, *Report 404531-F*, Texas Transportation Institute, Texas A&M University, College Station, Texas.

Buth, C.E., Wanda, L.M., and Schoeneman, S.K. (2000). "NCHRP Report 350 assessment of existing roadside safety hardware." FHWA Contract DTFH61-97-C-00039, *Report 404211-F*, Texas Transportation Institute, Texas A&M University, College Station, Texas.

Hallquist, J.O. (1998). *LS-DYNA Theoretical Manual*. Livermore Software Technology Company, Livermore, California.

Hypermesh 5.0 Documentation. (2001). Altair Computing, Inc., Troy, Michigan.

LS-DYNA Keyword User's Manual: Nonlinear Dynamic Analysis of Structures in Three Dimensions. (2001). Version 960, Volumes 1 and 2, Livermore Software Technology Company, Livermore, California.

LS-DYNA Theoretical Manual. (1998). Livermore Software Technology Company, Livermore, California.

Mak, K. K., and Menges, W. (1996). "Testing of state roadside safety systems, Volume VIII: Appendix G – Crash test and evaluation of the Single Sloped Bride Rail." *Report No. FHWA/RD-96/7147-Vol. VIII*, Texas Transportation Institute, Texas A&M University, College Station, Texas.

National Safety Council (NSC). (1998). *Accident facts.* Chicago, Illinois.

"Public finite element model archive: vehicle models." (2004). National Crash Analysis Center, Ashburn, Virginia. <http://www.ncac.gwu.edu/vml/models.html >.

Ross, H.E., Sicking, D. L., Zimmer, R. A., and Michie, J. D. (1993). "Recommended procedures for the safety performance evaluation of highway features." National Cooperative Highway Research Program *Report 350*, Transportation Research Board, Washington, D.C.

Ross, H. E. (1995). "Evolution of roadside safety." *Transportation Research Circular*, Transportation Research Board, Washington, D. C., 435(2), 5-16.

White, M., Jewell, J., and Peter, R. (2002). "Crash testing of various textured barriers." *Caltrans Research Report No. 65-680445*, California Department of Transportation, Sacramento, California.

APPENDIX I

SAMPLE LS-DYNA INPUT FILE

```
*KEYWORD
$$ HM_OUTPUT_DECK created 13:48:21 02-12-2004 by HyperMesh Version 6.0
$$ Ls-dyna Input Deck Generated by HyperMesh Version  : 6.0
$$ Generated using HyperMesh-Ls-dyna Template Version : 6.0
*TITLE
C1500 PICKUP TRUCK MODEL with Parametric System
*CONTROL_TERMINATION
$$  ENDTIM    ENDCYC     DTMIN    ENDENG    ENDMAS
       0.2
*CONTROL_OUTPUT
$$   NPOPT    NEECHO    NREFUP    IACCOP     OPIFS    IPNINT    IKEDIT
                   1
*CONTROL_ENERGY
$$    HGEN      RWEN    SLNTEN     RYLEN
         2
$$DATABASE_OPTION -- Control Cards for ASCII output
*DATABASE_NODOUT
5.0000E-04
*DATABASE_ELOUT
5.0000E-04
*DATABASE_GLSTAT
5.0000E-04
*DATABASE_MATSUM
5.0000E-04
*DATABASE_RCFORC
5.0000E-04
*DATABASE_SLEOUT
5.0000E-04
*DATABASE_BINARY_D3PLOT
$$ DT/CYCL      LCDT      BEAM     NPLTC
     0.005
*DATABASE_BINARY_D3DUMP
$$ DT/CYCL
   30000.0
*DATABASE_BINARY_RUNRSF
$$ DT/CYCL
   75000.0
*DATABASE_EXTENT_BINARY
$$   NEIPH     NEIPS    MAXINT    STRFLG    SIGFLG    EPSFLG    RLTFLG    ENGFLG

$$  CMPFLG    IEVERP    BEAMIP     DCOMP      SHGE     STSSZ    N3THDT
                   1
*NODE
 1000001 2959.27676203771518.45104495919           12.5
               ...
            Omitted for brevity
               ...
 111993913221.7836764597-3152.4541137855 222.11391347625
*MAT_RIGID
$HMNAME MATS   10001barrier
     100017.8600E-09  210000.0      0.28
       1.0
         0
*PART
$HMNAME COMPS   10001barrier
$HMCOLOR COMPS   10001      15

     10001     10001     10001
*SECTION_SHELL
$HMNAME PROPS   10001barrier
     10001        16                   0                 0.0
      10.0      10.0      10.0      10.0
*RIGIDWALL_PLANAR
$HMNAME GROUPS       1ground
$HMCOLOR GROUPS       1       1
$HMFLAG GROUPS SLAVE
         0
```

```
2959.276761518.45104       0.02959.276761518.45104       1.0       0.4
*ELEMENT_SHELL
 1118059   10001 1109919 1111616 1110362 1110362
               ...
            Omitted for brevity
               ...
 1125512   10001 1117312 1118921 1116818 1118030
$$
$$ Sets Defined In HyperMesh
$$
*BOUNDARY_SPC_NODE
$HMNAME LOADCOLS       1auto1
$HMCOLOR LOADCOLS       1       1
   1000011         0         1         1         1         1         1         1
   1000017         0         1         1         1         1         1         1
   1000073         0         1         1         1         1         1         1
   1000243         0         1         1         1         1         1         1
   1119881         0         1         1         1         1         1         1
   1117337         0         1         1         1         1         1         1
   1119930         0         1         1         1         1         1         1
   1116966         0         1         1         1         1         1         1
$*END
$*KEYWORD
$*TITLE
$ C1500 PICKUP TRUCK MODEL - (NCAC V4)
$*CONTROL_TERMINATION
$ 0.1500000         0 0.0000000         0 0.0000000
$*CONTROL_TIMESTEP
$ 0.0000000 0.0000000         0 0.0000000 0.0000000         0         0         0
$*CONTROL_SHELL
$ 90.000000         1         0         0         0         0         0
$*CONTROL_CONTACT
$ 0.0000000 0.0000000         0         2         0         0         0
$         0         0         0         0 0.0000000         0         0         0
$*CONTROL_PARALLEL
$         6         0         0
$*CONTROL_OUTPUT
$         1         3         0         0 0.0000000         0         0
$*CONTROL_ENERGY
$         0         0         0         0
$*DATABASE_BINARY_D3PLOT
$ 3.00000-3                   0
$*DATABASE_BINARY_D3THDT
$ 1.0000+10
$*DATABASE_BINARY_RUNRSF
$     10000
$*DATABASE_BINARY_INTFOR
$ 1.0000+10                   0
$*DATABASE_EXTENT_BINARY
$         0         0         0         0         2         2         2         2
$         0         1         0         0         0         0
$*DATABASE_RWFORC
$ 1.00000-4
$*DATABASE_NODOUT
$ 5.00000-5
$*DATABASE_GLSTAT
$ 1.00000-4
$*DATABASE_DEFORC
$ 1.00000-4
$*DATABASE_MATSUM
$ 5.00000-4
$*DATABASE_RCFORC
$ 1.00000-4
$*DATABASE_ABSTAT
$ 1.00000-4
$*DATABASE_SLEOUT
$ 1.00000-4
```

```
$*DATABASE_JNTFORC
$ 1.00000-4
$*CONTROL_CPU
$ 0.0000000
*MAT_PIECEWISE_LINEAR_PLASTICITY
         1 7.89000-9 2.10000+5 0.3000000 270.00000 0.0000000 1.00000+8 0.0000000
 0.0000000 0.0000000         0         0
 0.0000000 0.0487900 0.0953100 0.1398000 0.2231000 0.2624000 2.3980000 0.0000000
 270.00000 320.29999 366.29999 402.50000 438.79999 448.50000 449.00000 0.0000000
               ...
            Omitted for brevity
               ...
*MAT_RIGID
       224 7.89000-9 2.10000+5 0.3000000 0.0000000 0.0000000 0.0000000
 0.0000000 0.0000000 0.0000000
 0.0000000 0.0000000 0.0000000 0.0000000 0.0000000 0.0000000 0.0000000 0.0000000
*SECTION_SHELL
         1         2 0.0000000 4.0000000 0.0000000 0.0000000         0
      5.72      5.72      5.72      5.72 0.0000000
               ...
            Omitted for brevity
               ...
*SECTION_SOLID
       224         0
*PART
SHELL:       RAIL-FRONT-RIGHT-INNER
         1         1         1         0         0         0         0         0
               ...
            Omitted for brevity
               ...
*PART
SOLID:        ACCELEROMETER:  C.G.
       408       224       224         0         0         0         0         0
*NODE
       1 4.123851563E+03-9.361569214E+02 6.565278320E+02       0       0
               ...
            Omitted for brevity
               ...
  990802 3.086000000E+03 4.500000000E+01 1.369000000E+03       0       0
*ELEMENT_SOLID
   20000     103   20003   20001   20004   20005   20013   20010   20011   20012
               ...
            Omitted for brevity
               ...
  990008     408  990460  990461  990463  990462  990464  990465  990467  990466
*ELEMENT_BEAM
   66000     208   61552  901032   91344
               ...
            Omitted for brevity
               ...
  971057     205    8660    8663   91381
*ELEMENT_SHELL
       1      10     162       4       1       1
               ...
            Omitted for brevity
               ...
  985423     171  985176  985131  985125  985125
*DATABASE_HISTORY_NODE
    990747    990755    990763    990771    990779    990787    990795    990460
    990461
*DEFINE_CURVE
         1         0 0.0000000 0.0000000 0.0000000 0.0000000
      1.59999996E-01      2.00000000E+00
      2.00000003E-01      8.97000015E-01
      8.00000012E-01      8.96000028E-01
      1.00000000E+00      0.00000000E+00
*DEFINE_CURVE
         2         0 0.0000000 0.0000000 0.0000000 0.0000000
```

```
      0.00000000E+00      1.37500003E-01
      1.00000005E-03      1.37500003E-01
      1.09999999E-03      0.00000000E+00
      1.00000000E+00      0.00000000E+00
*DEFINE_CURVE
         3         0 0.0000000 0.0000000 0.0000000 0.0000000
      0.00000000E+00      0.00000000E+00
      1.00000005E-03      1.00000000E+00
      1.00000000E+00      1.00000000E+00
*CONSTRAINED_SPOTWELD
    105843    105655 0.0000000 0.0000000 0.0000000 0.0000000 0.0000000 0.0000000
                ...
            Omitted for brevity
                ...
*CONSTRAINED_SPOTWELD
     74752     77110 0.0000000 0.0000000 0.0000000 0.0000000 0.0000000 0.0000000
$
$       Changed 27982.166 to 27777.778 and 78.600 to 78.026
$
*INITIAL_VELOCITY_GENERATION
         1         1 0.0000000 27777.778 0.0000000 0.0000000
 0.0000000 0.0000000 0.0000000 0.0000000 1.0000000 0.0000000         0
*INITIAL_VELOCITY_GENERATION
         6         3 0.0000000 27777.778 0.0000000 0.0000000
 0.0000000 0.0000000 0.0000000 0.0000000 1.0000000 0.0000000         0
*INITIAL_VELOCITY_GENERATION
         2         1 78.026000 27777.778 0.0000000 0.0000000
 3640.2460 0.0000000  361.2287 0.0000000 1.0000000 0.0000000         0
*INITIAL_VELOCITY_GENERATION
         3         1 78.026000 27777.778 0.0000000 0.0000000
  275.5200 0.0000000  362.4570 0.0000000 1.0000000 0.0000000         0
*SET_PART_LIST
         1
         1         2         3         4         5         6         7         8
         9        10        11        12        13        14        15        16
        17        18        19        20        21        22        23        24
        25        26        27        28        29        30        31        32
        33        34        35        36        37        38        39        40
        41        42        43        44        45        46        47        48
        49        50        51        52        53        54        55        56
        57        58        59        60        61        62        63        64
        65        66        67        68        69        70        71        72
        73        74        75        76        77        78        79        80
        81        82        83        84        85        86        87        88
        89        90        91        92        93        94        95        96
        97        98        99       100       101       102       103       104
       105       106       107       108       109       110       111       112
       113       114       115       116       117       118       119       120
       121       122       123       124       125       126       127       128
       129       130       131       132       133       134       135       136
       137       138       139       140       141       142       143       144
       145       146       147       148       149       150       151       152
       153       154       155       156       157       158       159       160
       161       162       163       164       165       170       171       172
       173       174       175       176       177       178       179       180
       181       182       183       188       189       190       191       192
       193       194       195       196       197       198       199       200
       201       202       203       204       205       206       207       208
       209       214       215       216       401       402       403       404
       405       406       407       408
*SET_PART_LIST
         2
       184       185       186       187       210       211
*SET_PART_LIST
         3
       166       167       168       169       212       213
*SET_NODE_LIST
```

```
         6
     91344     91381     94460     94461     94462     94463     94464     94465
    101294    101295    101830    101831    101832    101833    101834    101835
    105197    510439    903453    903454    903455    903456    903457    903458
    903461    903462    903463    903464    903465    903466    906340    906341
    906344    906345    906346    906347    971495    971496    971497    971498
    982003    982004    982011    982012    982013    982014    982021    982022
    982031    982032    982033    982034    983100    983101    983102    983103
     94466     94467    101836    101837    903459    903460    906342    906343
    982001    982002    982023    982024    983104    983105
$ INTERFACE NAME: 1          $$$
*CONTACT_TIED_NODES_TO_SURFACE
         5         6         4         0         0         0         0         0
 0.0000000 0.0000000 0.0000000 0.0000000 0.0000000         0 0.0000000 0.0000000
 0.0000000 0.0000000 0.0000000 0.0000000 0.0000000 0.0000000
$ INTERFACE NAME: 2          $$$
*CONTACT_TIED_NODES_TO_SURFACE
         7         8         4         0         0         0         0         0
 0.0000000 0.0000000 0.0000000 0.0000000 0.0000000         0 0.0000000 0.0000000
 0.0000000 0.0000000 0.0000000 0.0000000 0.0000000 0.0000000
$*DEFINE_BOX
$         1-1.0000+10 1.0000+10-1.0000+10 1.0000+10-1.0000+10 1.0000+10
*SET_NODE_LIST
$
$$$ Slave nodes, surface:   1
$
         5
    105001    105002    105003    105004    105007    105008    105009    105010
    105025    105026    105027    105029    105030    105031    105033    105034
    105035    105048    105049    105050    105197    105563    105565    105566
    105567    105573    105583    105586    105693    105695    105696    105697
    105703    105713    105716    105779    105780    105781    105782    105783
    105784    105785    105786    105787    105788    105792    105793    105794
    105795    105796    105797    105798    105799    105800    105801    105802
    105803    105805    105807    105808    105809    105810    105811    105812
    105813    105814    105815    105816    105817    105818    105821    105822
    105823    105824    105825    105826    105827    105830    105831    105832
    105833    105834    105989    105990    105991    105992    105993    105994
    105995    105996    106002    106003    106004    106006    106007    106008
    106009    106010    106011    106012    106013    106016    106017    106018
    106019    106020    106021    106022    106023    106024    106025    106026
    106027    106028    106030    106031    106032    106033    106034    106035
    106036    106037    106040    106041    106042    106043    106044
*SET_SEGMENT
$
$ Master segments, surface:   1
$
         6
    105070    105071    105103    105101
               ...
            Omitted for brevity
               ...
    106948    106973    106974    106949
*SET_NODE_LIST
$
$$$ Slave nodes, surface:   2
$
         7
     22031     22032     22034     22035     22036     22037     22039     22040
     22230     22231     22232     22234     22235     22236     22237     22239
     22240     22241     23047     23048     23051     23243     23246     23247
     23248     23251     24097     24098     24099     24100     24101     24102
     24103     24104     24106     24108     24109     24110     24111     24113
     24114     24115     24116     25051     25052     25055     25056     25057
     25059     25060     81561     81562     81563     81564     81565     81567
     81568     81569     81570     81571     81572     81573     81574     81575
     81576     81577     81580     81581     81582     81583     81638     81639
```

```
     81642     81643     81646     81647
*SET_SEGMENT
$
$ Master segments, surface:   2
$
         8
     20003     20005     20004     20001
              ...
           Omitted for brevity
              ...
     81460     81461     81465     81459
*CONSTRAINED_RIGID_BODIES
       181       180
       179       178
       171       214
       171       215
       405       180
       406       178
*CONSTRAINED_EXTRA_NODES_SET
        21        10
*SET_NODE_LIST
        10
     70673     70674     70675     70705     71307     71308     71309     71489
     71491     71492     71493     71494     71513     71514     71515     71516
     71517     71535     71536     71540     71558     72946     72947     72948
     72949     72953     72954     72955     72959     72961     72992     72993
     73012     73017     73731     73733    903455    903456    903457    903458
              ...
           Omitted for brevity
              ...
*CONSTRAINED_EXTRA_NODES_SET
       408        47
*SET_NODE_LIST
        47
      7339      7340      7341      7344      7345      7346      7349      7350
      7351
*CONSTRAINED_JOINT_REVOLUTE
    903453    903456    101294    903455         0         0 0.0000000 0.0000000
*CONSTRAINED_JOINT_REVOLUTE
    101295    903457    903454    903458         0         0 0.0000000 0.0000000
*CONSTRAINED_JOINT_REVOLUTE
    903463    903465    903464    903466         0         0 0.0000000 0.0000000
*CONSTRAINED_JOINT_REVOLUTE
    903460    903462    903459    903461         0         0 0.0000000 0.0000000
*CONSTRAINED_JOINT_REVOLUTE
    101830    101832    101831    101833         0         0 0.0000000 0.0000000
*CONSTRAINED_JOINT_REVOLUTE
    101835    101837    101834    101836         0         0 0.0000000 0.0000000
*CONSTRAINED_JOINT_REVOLUTE
     94460     94462     94461     94463         0         0 0.0000000 0.0000000
*CONSTRAINED_JOINT_REVOLUTE
     94465     94467     94464     94466         0         0 0.0000000 0.0000000
*CONSTRAINED_JOINT_SPHERICAL
    906342    906343         0         0         0         0 0.0000000 0.0000000
*CONSTRAINED_JOINT_SPHERICAL
    906340    906341         0         0         0         0 0.0000000 0.0000000
*CONSTRAINED_JOINT_SPHERICAL
    906344    906345         0         0         0         0 0.0000000 0.0000000
*CONSTRAINED_JOINT_SPHERICAL
    906346    906347         0         0         0         0 0.0000000 0.0000000
*CONSTRAINED_JOINT_REVOLUTE
    982011    982012    982013    982014         0         0 0.0000000 0.0000000
*CONSTRAINED_JOINT_REVOLUTE
    982001    982002    982003    982004         0         0 0.0000000 0.0000000
*CONSTRAINED_JOINT_REVOLUTE
    982021    982022    982023    982024         0         0 0.0000000 0.0000000
*CONSTRAINED_JOINT_REVOLUTE
```

```
    982031    982032    982033    982034         0         0 0.0000000 0.0000000
*CONSTRAINED_JOINT_UNIVERSAL
    983100    983101    983030    984064         0         0 0.0000000 0.0000000
*CONSTRAINED_JOINT_UNIVERSAL
    983102    983103    983104    983105         0         0 0.0000000 0.0000000
*LOAD_BODY_Z
         3 9806.0000         0
*SECTION_DISCRETE
       409         0 0.0000000 0.0000000 0.0000000 0.0000000
 0.0000000 0.0000000
*MAT_SPRING_ELASTIC
       409 14.400000
*PART
Spring-Damper Part Definition.
       409       409       409
*SECTION_DISCRETE
       410         0 0.0000000 0.0000000 0.0000000 0.0000000
 0.0000000 0.0000000
*MAT_DAMPER_VISCOUS
       410 2.9349999
*PART
Spring-Damper Part Definition.
       410       410       410
*ELEMENT_DISCRETE
       1     409  971496  971498       0  0.00000000E+00       0  0.00000000E+00
       2     409  971497  971495       0  0.00000000E+00       0  0.00000000E+00
       3     410  971496  971498       0  0.00000000E+00       0  0.00000000E+00
       4     410  971497  971495       0  0.00000000E+00       0  0.00000000E+00
*ELEMENT_MASS
  971058   91344     1.00000E-06
           ...
      Omitted for brevity
           ...
  971127  983105     1.00000E-06
*ELEMENT_SEATBELT_ACCELEROMETER
         1    990747    990748    990749         0
         2    990755    990756    990757         0
         3    990763    990764    990765         0
         4    990771    990772    990773         0
         5    990779    990780    990781         0
         6    990787    990788    990789         0
         7    990795    990796    990797         0
         8    990460    990461    990462         0
*CONSTRAINED_NODAL_RIGID_BODY
        48         0
*SET_NODE_LIST
        48
    104247    104272    104614    104615    105038    105039    105043    105044
           ...
      Omitted for brevity
           ...
*CONSTRAINED_NODAL_RIGID_BODY
       907         0
*SET_NODE_LIST
       907
     71572     71574     71576     71578     73581     73584     73587     73590
     73593     73595     73719     73722    971498
*AIRBAG_SIMPLE_AIRBAG_MODEL_1
       908         1         0 0.0000000 0.0000000 0.0000000 0.0000000 0.0000000
 7.17000+8 1.00400+9 300.00000         2 0.7000000 0.0000000 0.1000000 1.2040-12
         0
*SET_PART_LIST
       908
       168
*AIRBAG_SIMPLE_AIRBAG_MODEL_2
       909         1         0 0.0000000 0.0000000 0.0000000 0.0000000 0.0000000
 7.17000+8 1.00400+9 300.00000         2 0.7000000 0.0000000 0.1000000 1.2040-12
```

```
         0
*SET_PART_LIST
       909
       169
*AIRBAG_SIMPLE_AIRBAG_MODEL_3
       910         1         0 0.0000000 0.0000000 0.0000000 0.0000000 0.0000000
 7.17000+8 1.00400+9 300.00000         2 0.7000000 0.0000000 0.1000000 1.2040-12
         0
*SET_PART_LIST
       910
       185
*AIRBAG_SIMPLE_AIRBAG_MODEL_4
       911         1         0 0.0000000 0.0000000 0.0000000 0.0000000 0.0000000
 7.17000+8 1.00400+9 300.00000         2 0.7000000 0.0000000 0.1000000 1.2040-12
         0
*SET_PART_LIST
       911
       187
*CONTACT_AUTOMATIC_SINGLE_SURFACE
         9         0         2         0         0         0         0         0
 0.0000000 0.0000000 0.0000000 0.0000000 0.0000000         0 0.0000000 0.0000000
 0.2000000 0.0000000 0.0000000 0.0000000 0.0000000 0.0000000
         2       0.1         0     1.025       5.0         5         0         1
       0.0         0         0         0
         2         0
*SET_PART
         9
         1         2         3         4         5         6         7         8
         9        10        11        12        13        14        15        16
        17        18        19        20        21        22        25        26
        28        29        30        31        32        33        36        37
        38        39        40        41        42        43        44        45
        46        47        48        49        50        51        52        53
        54        55        56        57        58        59        60        61
        62        63        64        65        66        68        69        70
        71        72        73        74        75        76        77        78
        79        80        81        82        83        84        85        86
        87        88        89        90        91        92        93        94
        95        96        97        98        99       104       105       106
       107       108       109       110       111       112       113       114
       115       116       117       118       119       120       121       122
       123       124       125       126       127       128       129       130
       131       132       133       134       135       136       137       138
       139       140       141       142       143       144       145       146
       147       148       149       154       155       156       157       158
       159       160       161       162       163       164       165       166
       167       168       169       174       175       176       177       178
       179       180       181       182       183       184       185       186
       187       196       197       198       199       200       207       209
       212       213
*CONTACT_SURFACE_TO_SURFACE
$HMNAME GROUPS      20Surf2Surf_18
$HMCOLOR GROUPS       20       1
       620       622         2         2
      0.15      0.15                                       1
       0.0       0.0       0.0       0.0       2.0       0.0
         2       0.1         0     1.025       0.0         2         0         1
       0.0         0         0         0
         2         0
*SET_PART_LIST
$HMSET
$HMNAME SETS     620Set_620
       620
         1         2         3         4         5         6         7         8
         9        10        11        12        13        14        15        16
        17        18        19        20        21        22        25        26
        28        29        30        31        32        33        36        37
```

```
       38        39        40        41        42        43        44        45
       46        47        48        49        50        51        52        53
       54        55        56        57        58        59        60        61
       62        63        64        65        66        68        69        70
       71        72        73        74        75        76        77        78
       79        80        81        82        83        84        85        86
       87        88        89        90        91        92        93        94
       95        96        97        98        99       104       105       106
      107       108       109       110       111       112       113       114
      115       116       117       118       119       120       121       122
      123       124       125       126       127       128       129       130
      131       132       133       134       135       136       137       138
      139       140       141       142       143       144       145       146
      147       148       149       154       155       156       157       158
      159       160       161       162       163       164       165       166
      168       174       175       176       177       178
      179       180       181       182       183       186
      187       196       197       198       199       200       207       209
      210       211       212       213
*CONTACT_FORCE_TRANSDUCER_PENALTY
$HMNAME GROUPS       6PForTrans_5
$HMCOLOR GROUPS       6       1
      621                   2                   1         0         0         0
1.0000E-031.0000E-03       0.0       0.0       0.0         1       0.0       0.0
      0.0       0.0       0.0       0.0       2.0       0.0
*SET_PART_LIST
$HMSET
$HMNAME SETS     621Set_621
      621
      184       185     10001
*SET_PART_LIST
$HMSET
$HMNAME SETS     621Set_621
      622
    10001
*CONTACT_SURFACE_TO_SURFACE
$HMNAME GROUPS      20Surf2Surf_18
$HMCOLOR GROUPS      20       1
      623     10001         2         3
     0.15      0.15                                    1
      0.0       0.0       0.0       0.0       2.0       0.0
        2       0.1         0     1.025       0.0         2         0         1
      0.0         0         0         0
        2         0
*SET_PART_LIST
$HMSET
$HMNAME SETS     621Set_621
      623
      184       185       167       169
*CONTACT_FORCE_TRANSDUCER_PENALTY
$HMNAME GROUPS       6PForTrans_5
$HMCOLOR GROUPS       6       1
      624                   2                   1         0         0         0
1.0000E-031.0000E-03       0.0       0.0       0.0         1       0.0       0.0
      0.0       0.0       0.0       0.0       2.0       0.0
*SET_PART_LIST
$HMSET
$HMNAME SETS     621Set_621
      624
      185        54
*END
```

VITA

Jacob Raymond Ness received his B.S. degree in civil engineering with an emphasis on structures from Texas A&M University in December 2002. Immediately after graduating, he began work at Texas A&M University towards an M.S. degree in civil engineering. During this time, he worked as a research assistant at the Texas Transportation Institute (TTI) starting in February 2002. While employed by TTI, he studied the impact performance of roadside safety structures using finite element analysis. The results of the finite element analysis were used to design roadside safety devices to be tested using full-scale, high-speed crash tests. Completed models include portable concrete barriers and proprietary crash cushions. Upon completion of the M.S. degree, Mr. Ness will be employed by Matrix Structural Engineers in Houston, Texas. He will perform structural design and analysis of commercial structures. Mr. Ness can be contacted at:

C/o Joseph Ness

8239 Campobello Drive

San Antonio, TX 78218

(210) 590-8447